R. A. (2002) *Mol. Biol. Cell* **13,** 71–83
14. Chen, X., Van Valkenburgh, C., Fang, H., and Green, N. (1999) *J. Biol. Chem.* **274,** 37750–37754
15. Graham, B. H., Waymire, K. G., Cottrell, B., Trounce, I. A., MacGregor, G. R., and Wallace, D. C. (1997) *Nat. Genet.* **16,** 226–234
16. Hasegawa, K., Meyers, M. B., and Kitsis, R. N. (1997) *J. Biol. Chem.* **272,** 20049–20054
17. Nakagawa, M., Takemura, G., Kanamori, H., Goto, K., Maruyama, R., Tsujimoto, A., Ohno, T., Okada, H., Ogino, A., Esaki, M., Miyata, S., Li, L., Ushikoshi, H., Aoyama, T., Kawasaki, M., Nagashima, K., Fujiwara, T., Minatoguchi, S., and Fujiwara, H. (2008) *Circ. Res.* **103,** 98–106
18. Yanazume, T., Hasegawa, K., Morimoto, T., Kawamura, T., Wada, H., Matsumori, A., Kawase, Y., Hirai, M., and Kita, T. (2003) *Mol. Cell. Biol.* **23,** 3593–3606
19. Passarella, S., Ostuni, A., Atlante, A., and Quagliariello, E. (1988) *Biochem. Biophys. Res. Commun.* **156,** 978–986
20. Dörner, A., and Schultheiss, H. P. (2007) *Trends Cardiovasc. Med.* **17,** 284–290
21. Cimmino, A., Calin, G. A., Fabbri, M., Iorio, M. V., Ferracin, M., Shimizu, M., Wojcik, S. E., Aqeilan, R. I., Zupo, S., Dono, M., Rassenti, L., Alder, H., Volinia, S., Liu, C. G., Kipps, T. J., Negrini, M., and Croce, C. M. (2005) *Proc. Natl. Acad. Sci. U.S.A.* **102,** 13944–13949
22. Das, A. M., and Harris, D. A. (1990) *Biochem. J.* **266,** 355–361
23. Soubannier, V., and McBride, H. M. (2009) *Biochim. Biophys. Acta* **1793,** 154–170
24. Schaper, J., Froede, R., Hein, S., Buck, A., Hashizume, H., Speiser, B., Friedl, A., and Bleese, N. (1991) *Circulation* **83,** 504–514
25. Sabbah, H. N., Sharov, V., Riddle, J. M., Kono, T., Lesch, M., and Goldstein, S. (1992) *J. Mol. Cell. Cardiol.* **24,** 1333–1347
26. Ning, X. H., Zhang, J., Liu, J., Ye, Y., Chen, S. H., From, A. H., Bache, R. J., and Portman, M. A. (2000) *J. Am. Coll. Cardiol.* **36,** 282–287
27. Taguchi, N., Ishihara, N., Jofuku, A., Oka, T., and Mihara, K. (2007) *J. Biol. Chem.* **282,** 11521–11529
28. Zunino, R., Schauss, A., Rippstein, P., Andrade-Navarro, M., and McBride, H. M. (2007) *J. Cell Sci.* **120,** 1178–1188
29. Duisters, R. F., Tijsen, A. J., Schroen, B., Leenders, J. J., Lentink, V., van der Made, I., Herias, V., van Leeuwen, R. E., Schellings, M. W., Barenbrug, P., Maessen, J. G., Heymans, S., Pinto, Y. M., and Creemers, E. E. (2009) *Circ. Res.* **104,** 170–178, 6p following 178
30. Ebert, M. S., Neilson, J. R., and Sharp, P. A. (2007) *Nat. Methods* **4,** 721–726
31. Bhamidipati, A., Lewis, S. A., and Cowan, N. J. (2000) *J. Cell Biol.* **149,** 1087–1096
32. Dörner, A., Olesch, M., Giessen, S., Pauschinger, M., and Schultheiss, H. P. (1999) *Biochim. Biophys. Acta* **1417,** 16–24
33. Dolce, V., Scarcia, P., Iacopetta, D., and Palmieri, F. (2005) *FEBS Lett.* **579,** 633–637
34. Levy, S. E., Chen, Y. S., Graham, B. H., and Wallace, D. C. (2000) *Gene* **254,** 57–66
35. Stepien, G., Torroni, A., Chung, A. B., Hodge, J. A., and Wallace, D. C. (1992) *J. Biol. Chem.* **267,** 14592–14597
36. Wallace, D. C. (2001) *Am. J. Med. Genet.* **106,** 71–93
37. Murdock, D. G., Boone, B. E., Esposito, L. A., and Wallace, D. C. (1999) *J. Biol. Chem.* **274,** 14429–14433
38. Jordens, E. Z., Palmieri, L., Huizing, M., van den Heuvel, L. P., Sengers, R. C., Dörner, A., Ruitenbeek, W., Trijbels, F. J., Valsson, J., Sigfusson, G., Palmieri, F., and Smeitink, J. A. (2002) *Ann. Neurol.* **52,** 95–99

nature neuroscience

Nardilysin regulates axonal maturation and myelination in the central and peripheral nervous system

Mikiko Ohno[1], Yoshinori Hiraoka[1], Tatsuhiko Matsuoka[1], Hidekazu Tomimoto[2], Keizo Takao[3–5], Tsuyoshi Miyakawa[3–5], Naoko Oshima[6], Hiroshi Kiyonari[6], Takeshi Kimura[1], Toru Kita[1,7] & Eiichiro Nishi[1]

Axonal maturation and myelination are essential processes for establishing an efficient neuronal signaling network. We found that nardilysin (N-arginine dibasic convertase, also known as Nrd1 and NRDc), a metalloendopeptidase enhancer of protein ectodomain shedding, is a critical regulator of these processes. *Nrd1*$^{-/-}$ mice had smaller brains and a thin cerebral cortex, in which there were less myelinated fibers with thinner myelin sheaths and smaller axon diameters. We also found hypomyelination in the peripheral nervous system (PNS) of *Nrd1*$^{-/-}$ mice. Neuron-specific overexpression of NRDc induced hypermyelination, indicating that the level of neuronal NRDc regulates myelin thickness. Consistent with these findings, *Nrd1*$^{-/-}$ mice had impaired motor activities and cognitive deficits. Furthermore, NRDc enhanced ectodomain shedding of neuregulin1 (NRG1), which is a master regulator of myelination in the PNS. On the basis of these data, we propose that NRDc regulates axonal maturation and myelination in the CNS and PNS, in part, through the modulation of NRG1 shedding.

Myelination of axons by glial cells, such as oligodendrocytes in the CNS and Schwann cells in the PNS, is essential for rapid impulse conduction. Myelination is coordinated by the interaction between axons and glial cells. Although the diameter of an axon dictates whether myelination is initiated, myelination may further induce radial growth of axons[1,2]. Because axonal conduction is determined by axon caliber and myelin sheath thickness, axonal maturation (radial growth of axon) and myelination are essential processes for establishing an efficient neuronal signaling network[3,4]. Several lines of evidence suggest that bidirectional signaling between axons and myelin maintains neuronal functions. For example, some oligodendrocyte-specific proteins, such as proteolipid protein and 2′,3′-cyclic nucleotide phosphodiesterase (CNP), are required to maintain axonal integrity[5,6]. On the other hand, NRG1, a member of the epidermal growth factor (EGF) family, induces axonal signaling and is required for glial differentiation, proliferation and myelination[7–9]. NRG1 is synthesized as a transmembrane protein and then shed from the cell surface by proteolytic cleavage in the juxtamembrane region[10]. ADAM proteases and BACE1 (β-secretase) have been proposed as sheddases for NRG1 (refs. 11–15). Because BACE1-deficient mice have a hypomyelination phenotype[13–15], shedding of NRG1 is thought to be important in myelination *in vivo*. However, the underlying mechanism by which NRG1 shedding is regulated is poorly understood.

NRDc is a zinc peptidase of the M16 family that selectively cleaves dibasic sites[16,17]. We identified NRDc as a specific binding partner of heparin-binding EGF-like growth factor (HB-EGF) and found that NRDc enhances HB-EGF shedding through activation of tumor necrosis factor α converting enzyme (TACE, also known as ADAM17)[18,19]. We also found that NRDc enhances the ectodomain shedding of multiple membrane proteins, including amyloid precursor protein (APP) and tumor necrosis factor-α, through activation of several ADAM proteases[20,21]. These results suggest that NRDc may regulate the ectodomain shedding of a wide range of membrane proteins. To explore the physiological functions of NRDc, we generated *Nrd1*$^{-/-}$ mice and found that these mice had impaired axonal maturation and hypomyelination in both the CNS and PNS. Furthermore, we found that NRDc regulates axonal maturation and myelination in the CNS and PNS, in part, through the modulation of NRG1 shedding.

RESULTS

Small brains in *Nrd1*$^{-/-}$ mice

NRDc was highly expressed in brain lysates of early postnatal mice but was expressed at a lower level in the brains of adult mice (**Fig. 1a**). Using immunohistochemical analysis, we found that NRDc was expressed in neurons and dendrites but not in glial cells (**Fig. 1b**)[20]. These findings were supported by *in situ* hybridization, which revealed that there was little or no *Nrd1* mRNA in the corpus callosum (**Supplementary Fig. 1**).

To examine the physiological functions of NRDc, we generated *Nrd1*$^{-/-}$ mice by gene targeting (**Supplementary Fig. 2**). No *Nrd1* mRNA or protein was detected by real-time PCR (data not shown) and western blot analysis, respectively, in the brains (**Fig. 1a**) and all other

[1]Department of Cardiovascular Medicine, Graduate School of Medicine, Kyoto University, Sakyo-ku, Kyoto, Japan. [2]Department of Neurology, Graduate School of Medicine, Mie University, Tsu, Japan. [3]Division of Systems Medical Science, Institute for Comprehensive Medical Science, Fujita Health University, Toyoake, Aichi, Japan. [4]Japan Science and Technology Agency (JST), Institute for Bioinformatics Research and Development and Core Research for Evolutional Science and Technology, Kawaguchi, Saitama, Japan. [5]Frontier Technology Center, Graduate School of Medicine, Kyoto University, Sakyo-ku, Kyoto, Japan. [6]Laboratory for Animal Resources and Genetic Engineering, Center for Developmental Biology, RIKEN Kobe, Chuo-ku, Kobe, Japan. [7]Present address: Kobe City Medical Center General Hospital, Chuo-ku, Kobe, Japan. Correspondence should be addressed to E.N. (nishi@kuhp.kyoto-u.ac.jp).

Received 29 July; accepted 22 September; published online 22 November 2009; doi:10.1038/nn.2438

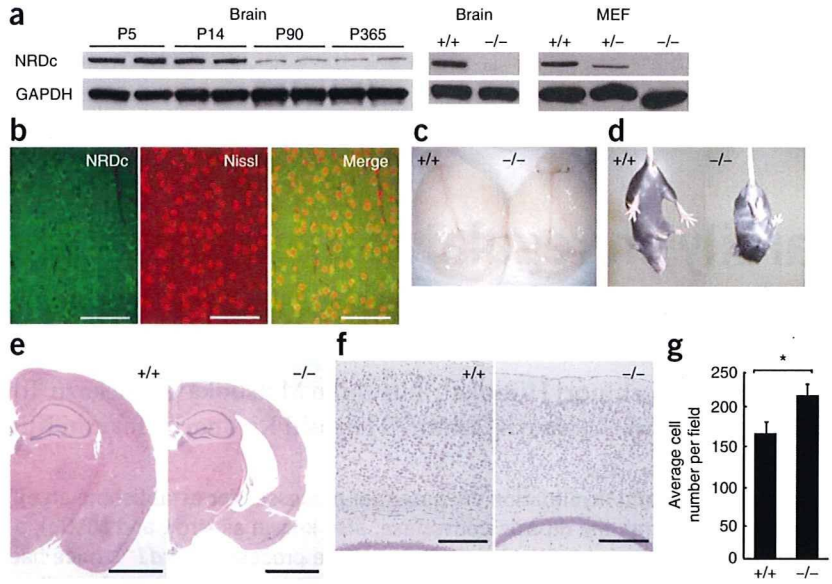

Figure 1 Expression of NRDc in brains and gross CNS phenotypes of *Nrd1*$^{-/-}$ mice. (**a**) Immunoblot analysis of brain extracts (left, center) or total cell extracts (right) stained with antibodies to NRDc and GAPDH. Analysis of brain extracts from wild-type mice at P5, P14, P90 and P365 (left) and from control wild-type (+/+) and *Nrd1*$^{-/-}$ mice (−/−) at P90 (center). Analysis of the total extracts of MEFs isolated from *Nrd1*$^{+/+}$, *Nrd1*$^{+/-}$ or *Nrd1*$^{-/-}$ mice (right). Full-length blots are presented in **Supplementary Figure 9**. (**b**) Immunohistochemistry using an antibody to NRDc (green) with cerebral cortex sections from wild-type mice at P30. The section was double-stained with fluorescent Nissl (red). Scale bars represent 250 μm. (**c**) Brains of *Nrd1*$^{-/-}$ mice and control wild-type littermates at P90. (**d**) Enhanced limb-clasping reflex of *Nrd1*$^{-/-}$ compared with wild-type mice at P42. (**e**) Hematoxylin and eosin–stained sections of one brain hemisphere of *Nrd1*$^{-/-}$ mice and wild-type littermates at P90. An enlargement of the lateral ventricles and cortical shrinkage in *Nrd1*$^{-/-}$ brain is shown. Scale bars represent 2 mm. (**f**,**g**) Nissl-stained sections of cerebral cortex of *Nrd1*$^{-/-}$ mice and wild-type littermates at P90. Scale bars represent 500 μm. Counting of Nissl-positive neurons at the same bregma levels (six non-overlapping fields, $n = 2$ per genotype, results are mean ± s.e.m., * $P < 0.01$) revealed that there was a greater neuronal cell density in the *Nrd1*$^{-/-}$ cortex.

tissues tested from *Nrd1*$^{-/-}$ mice (data not shown). Immunostaining of tissue sections also showed a lack of NRDc protein in the cerebral cortex of *Nrd1*$^{-/-}$ mice (**Supplementary Fig. 2**). The levels of NRDc protein in embryonic fibroblasts (MEFs) isolated from *Nrd1*$^{+/+}$, *Nrd1*$^{+/-}$ or *Nrd1*$^{-/-}$ mice correlated with the predicted gene dosage of *Nrd1* in these mice (**Fig. 1a**).

Pups lacking NRDc were born at the expected Mendelian ratio. However, approximately 80% died within 48 h of birth. *Nrd1*$^{-/-}$ pups weighed approximately 30% less than *Nrd1*$^{+/+}$ and *Nrd1*$^{+/-}$ littermates, indicating that NRDc is indispensable for normal prenatal growth. The *Nrd1*$^{-/-}$ mice that survived remained smaller than their wild-type and heterozygous littermates throughout postnatal development and had average brain weights that were 29% lower than those of *Nrd1*$^{+/+}$ mice at postnatal day 90 (P90) (*Nrd1*$^{+/+}$, 521.0 ± 30.0 mg; *Nrd1*$^{-/-}$, 371.5 ± 16.8 mg; $n = 5$, $P < 0.001$; **Fig. 1c**). Although the *Nrd1*$^{-/-}$ mice that survived lived until 2 years of age, they had several prominent neurological disorders. For example, *Nrd1*$^{-/-}$ mice exhibited enhanced limb-clasping reflexes when suspended by the tail, whereas control mice extended their limbs (**Fig. 1d**).

To assess the underlying neuropathology, we examined the brains of *Nrd1*$^{-/-}$ mice histologically. Although the gross anatomy of the *Nrd1*$^{-/-}$ mouse brain was normal at P1, P14 and P30 (**Supplementary Fig. 3**), we observed a thin cerebral cortex and enlarged lateral ventricles at P90 (**Fig. 1e**). We found that the *Nrd1*$^{-/-}$ cortex had a greater neuronal cell density than in the *Nrd1*$^{+/+}$ cortex by Nissl staining (**Fig. 1f,g**). Furthermore, there were no differences in the number of TUNEL-positive cells detected in the cortex of *Nrd1*$^{+/+}$ and *Nrd1*$^{-/-}$ mice (data not shown), indicating that there was no excessive loss of neurons in the *Nrd1*$^{-/-}$ cortex.

Hypomyelination in the CNS of *Nrd1*$^{-/-}$ mice

We next examined the integrity of axons and myelin using silver impregnation and luxol fast blue (LFB) staining, respectively. We detected much less silver impregnation in *Nrd1*$^{-/-}$ brains, especially in the corpus callosum and cortical layers adjacent to it

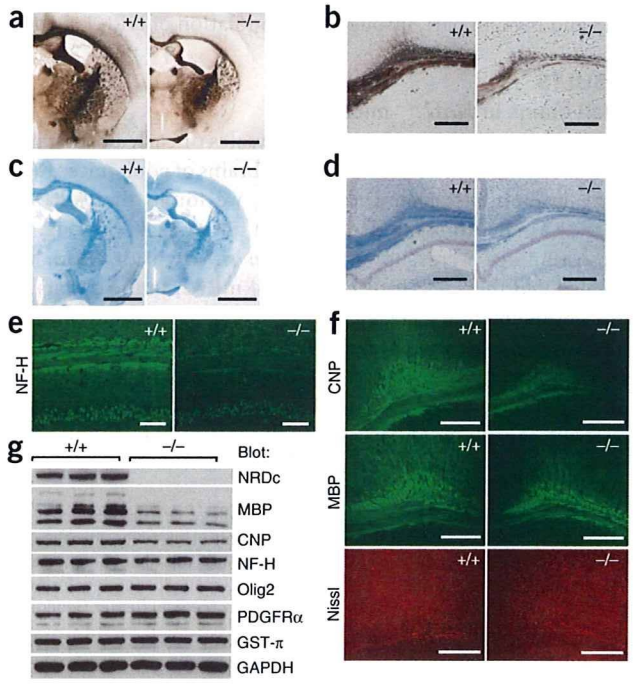

Figure 2 Impaired axonal maturation and hypomyelination in the CNS of *Nrd1*$^{-/-}$ mice. (**a**–**d**) Silver impregnation by Bielschowskey method (**a**,**b**) and LFB staining (**c**,**d**) of *Nrd1*$^{-/-}$ brain (−/−) and wild-type brain (+/+) at P90. We found impairment of axonal maturation and hypomyelination in *Nrd1*$^{-/-}$ brains, especially in the corpus callosum. (**e**,**f**) Immunohistochemistry using antibodies to NF-H (**e**), CNP and MBP (**f**) of corpus callosum from control wild-type mice and *Nrd1*$^{-/-}$ mice at P30. Scale bars represent 2 mm (**a**,**c**), 500 μm (**b**,**d**,**f**) and 250 μm (**e**). (**g**) Immunoblot analysis of brain extracts from wild-type and *Nrd1*$^{-/-}$ brains at P14 showed a reduction of MBP, CNP and NF-H expression in *Nrd1*$^{-/-}$ brains. On the other hand, there were no differences in Olig2, PDGFRα and GST-π expression ($n = 3$ in each genotype). Full-length blots are presented in **Supplementary Figure 9**.

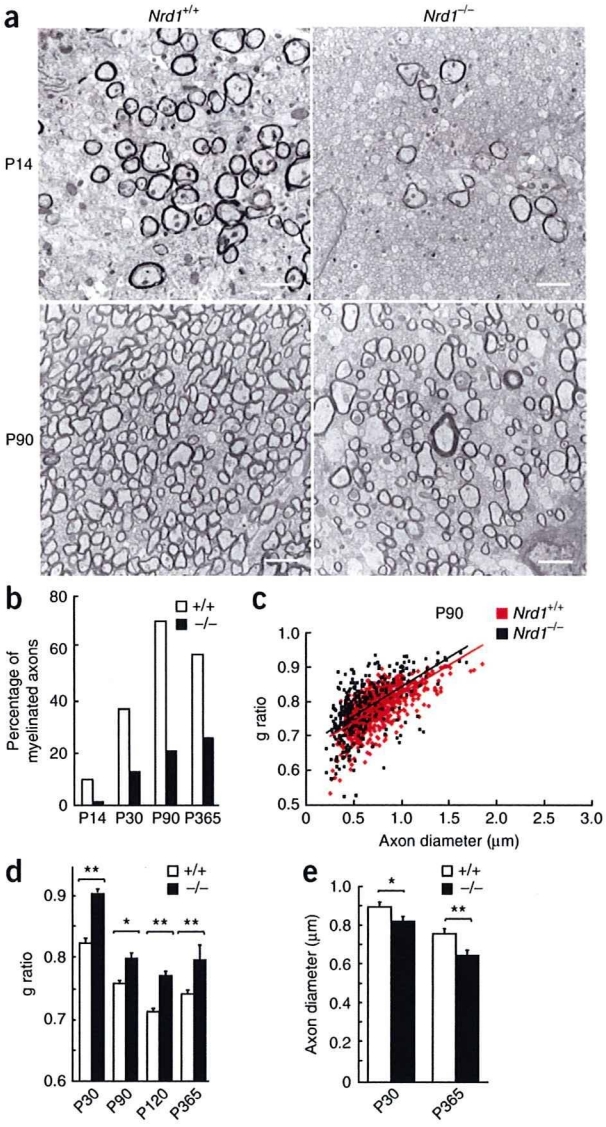

Figure 3 Delay in the initiation of myelination and hypomyelination in *Nrd1*$^{-/-}$ mice. Electron microscopic analysis of corpus callosum. (**a**) Electron micrographs of transverse sections at the corpus callosum from *Nrd1*$^{-/-}$ mice and wild-type littermates at P14 and P90. Scale bars represent 2 μm. (**b**) Percentage of myelinated axons in the corpus callosum of *Nrd1*$^{-/-}$and wild-type littermates at P14, P30, P90 and P365. (**c**,**d**) Quantitation of myelin sheath thickness in the corpus callosum by analyzing g ratios with electron micrographs. Scatter plots of myelin thickness, expressed as g ratios, against axon diameters at P90 in *Nrd1*$^{-/-}$ (black) and wild-type (red) corpus callosum are shown (**c**). We determined the average myelin sheath thickness (g ratio) of myelinated fibers at P30, P90, P120 and P365 and found hypomyelination in the corpus callosum of *Nrd1*$^{-/-}$ mice (**d**). Data represent the mean ± s.e.m. for 300–900 myelinated fibers from each group. * $P < 0.03$ and ** $P < 0.0001$. (**e**) Average diameters of myelinated axons in the corpus callosum at P30 and P365. Data represent the mean ± s.e.m. for 300–900 myelinated fibers from each group. * $P = 0.0002$ and ** $P < 0.0001$.

(**Fig. 2a**,**b**). Similarly, LFB staining was markedly weaker in this region (**Fig. 2c**,**d**). These results suggest that the volume of axons and myelin in *Nrd1*$^{-/-}$ brain is decreased, especially in the corpus callosum. Furthermore, expression of the axonal marker neurofilament-H (NF-H; **Fig. 2e**) and the myelin markers CNP and myelin basic protein (MBP) (**Fig. 2f**) were lower in the corpus callosum in *Nrd1*$^{-/-}$ brain at P30. Using western blotting, we found reduced CNP and MBP protein levels at an earlier stage (P14) in *Nrd1*$^{-/-}$ brain extracts (**Fig. 2g**), suggesting that *Nrd1*$^{-/-}$ mice have a severe impairment of axonal maturation and hypomyelination starting at the early stages of these processes. Neuronal expression of NRDc was detected in whole regions of the brain, but there were some prominent regional differences. For example, NRDc was highly expressed in cortical neurons, but neurons in striatum expressed relatively low levels of NRDc (**Supplementary Fig. 4**), similar to the expression pattern seen in human brain[22]. Consistent with these results, the myelination defect in *Nrd1*$^{-/-}$ striatum was not as obvious as the defect in the cortex, hippocampus and corpus callosum (**Supplementary Fig. 4**). These results suggest that there is a correlation between the expression level of NRDc and the extent of the myelination defect in *Nrd1*$^{-/-}$ mice.

On the other hand, western blots of the same set of brain extracts revealed that the expression of platelet-derived growth factor receptor α (PDGFRα) and oligodendrocyte transcription factor 2 (Olig2)[23], markers of oligodendrocyte precursors, and GST-π, a marker of mature oligodendrocyte, were not reduced in *Nrd1*$^{-/-}$ mice (**Fig. 2g**), suggesting that oligodendroglial differentiation is normal in *Nrd1*$^{-/-}$ mice. Moreover, we found via quantitative analysis of Olig2-positive cells at embryonic day 18.5 (E18.5) and P5 that there were no differences in the number of oligodendrocyte precursors in *Nrd1*$^{+/+}$ and *Nrd1*$^{-/-}$ brains (**Supplementary Fig. 5**). These data suggest that NRDc affects myelination, but not differentiation of oligodendrocytes.

To obtain direct evidence of impaired axonal maturation and hypomyelination in the CNS, we analyzed sections of the corpus callosum in *Nrd1*$^{-/-}$ mice and *Nrd1*$^{+/+}$ littermates between P14 and P365 by electron microscopy (**Fig. 3a** and **Supplementary Fig. 6**). The proportion of myelinated axons was markedly reduced in *Nrd1*$^{-/-}$ mice at all of the stages examined (**Fig. 3b**). At P14, only about one seventh of the *Nrd1*$^{-/-}$ axons were myelinated compared with the *Nrd1*$^{+/+}$ axons, indicating that there was a substantial delay in the initiation of myelination in *Nrd1*$^{-/-}$ mice. The proportion of myelinated axons in the *Nrd1*$^{-/-}$ CNS was only 21.0% at P90 and did not approach the level seen in *Nrd1*$^{+/+}$ mice even at P365 (**Fig. 3b**). We next compared myelin sheath thickness in the *Nrd1*$^{-/-}$ and *Nrd1*$^{+/+}$ corpus callosum by determining the g ratio[24] (axon diameter to total fiber diameter) of myelinated fibers at P30, P90, P120 and P365 (**Fig. 3c** and **Supplementary Fig. 6**). The average g ratios were higher in *Nrd1*$^{-/-}$ mice at all stages (**Fig. 3d**), indicating that myelin sheaths were thinner in *Nrd1*$^{-/-}$ mice compared with those of *Nrd1*$^{+/+}$ mice. The average diameters of myelinated axons were also smaller in *Nrd1*$^{-/-}$ mice than wild-type littermates (**Fig. 3e**). Although axons were hypomyelinated, the ultrastructure of myelin sheaths of *Nrd1*$^{-/-}$ mice appeared to be normal and indistinguishable from those of *Nrd1*$^{+/+}$ mice (data not shown). Together, these data indicate that *Nrd1*$^{-/-}$ mice have fewer myelinated fibers in the corpus callosum, and the fibers have thinner myelin sheaths and smaller axon diameters. As NRDc is highly expressed in neurons, but either not expressed or expressed at very low levels in glial cells (**Fig. 1b** and **Supplementary Fig. 4**)[20], we propose that the loss of NRDc in neurons may cause an impairment of axonal maturation, resulting in the perturbation of axonal signaling required for oligodendrocytes to properly myelinate axons and hypomyelination.

Hypomyelination in the PNS of *Nrd1*$^{-/-}$ mice

NRDc was also expressed in spinal neurons and dorsal root ganglion neurons (**Supplementary Fig. 1**). To investigate the role of NRDc in

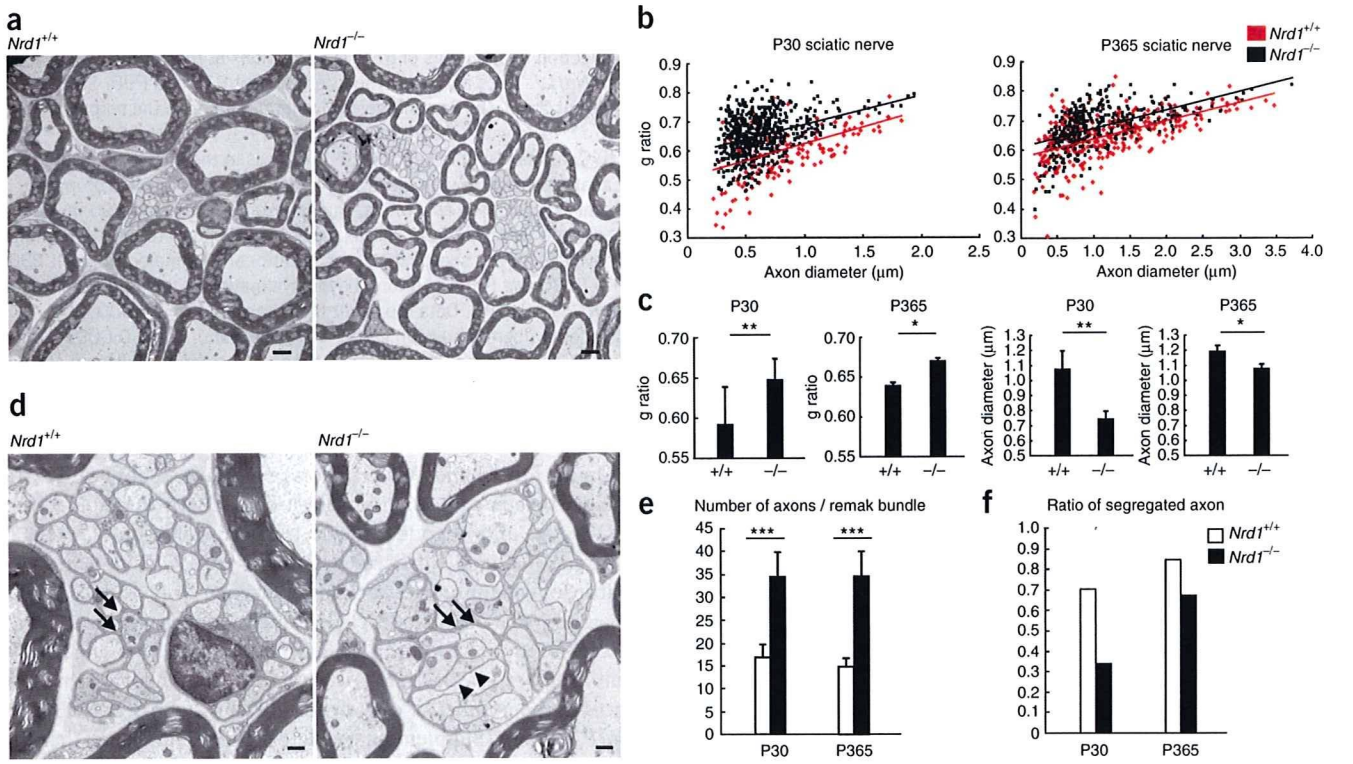

Figure 4 Impaired axonal maturation and hypomyelination in the PNS of *Nrd1*$^{-/-}$ mice. (**a**) Electron micrographs of sciatic nerves of *Nrd1*$^{+/+}$ and *Nrd1*$^{-/-}$ mice at P365 showed obvious hypomyelination in the *Nrd1*$^{-/-}$ nerves. Scale bars represent 2 μm. (**b**) Scatter plots of g ratios and axon diameters at P30 and P365 of *Nrd1*$^{-/-}$ and wild-type sciatic nerves. (**c**) G ratios and axon diameters at P30 and P365 of *Nrd1*$^{+/+}$ and *Nrd1*$^{-/-}$ sciatic nerves. Data represent the mean ± s.e.m. for 750 myelinated fibers from each group ($n = 4$ for each genotype). * $P < 0.03$ and ** $P < 0.01$. (**d**) Electron micrographs of Remak bundles in sciatic nerves showed altered axonal segregation in *Nrd1*$^{-/-}$ bundles. Arrows indicate Schwann cell cytoplasmic processes between different axons. Note that many axons of *Nrd1*$^{-/-}$ bundles are directly apposed without the cytoplasmic processes (arrowhead). Scale bars represent 500 nm. (**e**) The average numbers of axons in a Remak bundle at P30 and P365 were significantly reduced in *Nrd1*$^{-/-}$ sciatic nerves. Data represent the mean ± s.e.m. for 150–300 Remak bundle from each group ($n = 2$ for each genotype). *** $P < 0.0001$. (**f**) Ratios of segregated axons in *Nrd1*$^{-/-}$ sciatic nerves at P30 and P365 were reduced (150–300 Remak bundle from each group, $n = 2$ for each genotype).

axonal maturation and myelination in the PNS, we analyzed the sciatic nerves of *Nrd1*$^{-/-}$ mice by electron microscopy and found that the sciatic nerves of *Nrd1*$^{-/-}$ mice were hypomyelinated (**Fig. 4a**). Quantitative analysis by measuring the g ratio of myelinated fibers indicated that the myelin sheath thickness was thinner in *Nrd1*$^{-/-}$ mice at both P30 and P365. The diameter of myelinated axons was also smaller in *Nrd1*$^{-/-}$ nerves compared with *Nrd1*$^{+/+}$ nerves (**Fig. 4b,c**).

We also examined the morphology of Remak bundles (**Fig. 4d–f**). Remak bundles in *Nrd1*$^{-/-}$ nerves contained approximately two-fold more axons than *Nrd1*$^{+/+}$ nerves at P30 and P365 (**Fig. 4d,e**). In addition, there were many unsegregated or poorly segregated axons that lacked intervening Schwan cell processes in *Nrd1*$^{-/-}$ bundles (**Fig. 4d,f**). These findings indicate that NRDc is critical for axonal maturation and myelination of both the CNS and PNS. Notably, the observed hypomyelination and morphological changes of Remak bundles in the PNS of *Nrd1*$^{-/-}$ mice were very similar to those described in *Nrg1*$^{+/-}$ and *Bace1*$^{-/-}$ mice[7,8,13,14,25].

The level of neuronal NRDc regulates myelin thickness

To determine the dose-dependent effects of NRDc expression on the CNS phenotypes, we examined brains from *Nrd1*$^{+/-}$ mice, in which NRDc expression was obviously reduced (**Fig. 5a**). The gross anatomy of *Nrd1*$^{+/-}$ brains showed no cortical shrinkage, but we did find enlarged lateral ventricles (**Fig. 5b**). Although we detected no obvious differences between *Nrd1*$^{+/+}$ and *Nrd1*$^{+/-}$ brains by LFB staining (**Fig. 5b,c**), we did find decreased expression of the myelin and axon markers MBP and NF-H in *Nrd1*$^{+/-}$ corpus callosum by immunostaining (**Fig. 5d,e**). These findings were confirmed by western blot using whole brain lysates (**Fig. 5f**). Furthermore, we analyzed *Nrd1*$^{+/-}$ corpus callosum by electron microscopy and found that the myelin sheath thickness of *Nrd1*$^{+/-}$ mice was significantly thinner than that of *Nrd1*$^{+/+}$ mice (average g ratio: *Nrd1*$^{+/+}$, 0.725 ± 0.020 s.e.m.; *Nrd1*$^{+/-}$, 0.761 ± 0.001 s.e.m.; $n > 1000$ fibers from each group, $P < 0.0001$; **Fig. 5g,h**). The axon diameters of *Nrd1*$^{+/-}$ mice were also smaller compared with those of *Nrd1*$^{+/+}$ mice (*Nrd1*$^{+/+}$, 0.650 ± 0.018 μm; *Nrd1*$^{+/-}$, 0.582 ± 0.006 μm; $P < 0.0001$). Thus, *Nrd1*$^{+/-}$ mice have a CNS phenotype that is intermediate of those of *Nrd1*$^{+/+}$ and *Nrd1*$^{-/-}$ mice, indicating that the level of NRDc expression in neurons affects axonal maturation and myelination.

Our loss-of-function approach using *Nrd1*$^{-/-}$ mice revealed that NRDc is essential for axonal maturation and myelination in the CNS. To further define the role of NRDc in these processes, we used a gain-of-function approach with transgenic mice that overexpress mouse NRDc under the control of the *Camk2a* promoter (NRDc-Tg mice)[26,27]. Western blot analysis of whole brain extract of NRDc-Tg mice at P90 revealed that there was an increase in NRDc expression in the transgenic mice (**Fig. 6a**). The *Camk2a* promoter was specifically activated in neurons of cerebral cortex and hippocampus[26,27], where the increased expression of NRDc was confirmed by immunostaining (**Fig. 6b,c**). To see the regional effect of NRDc

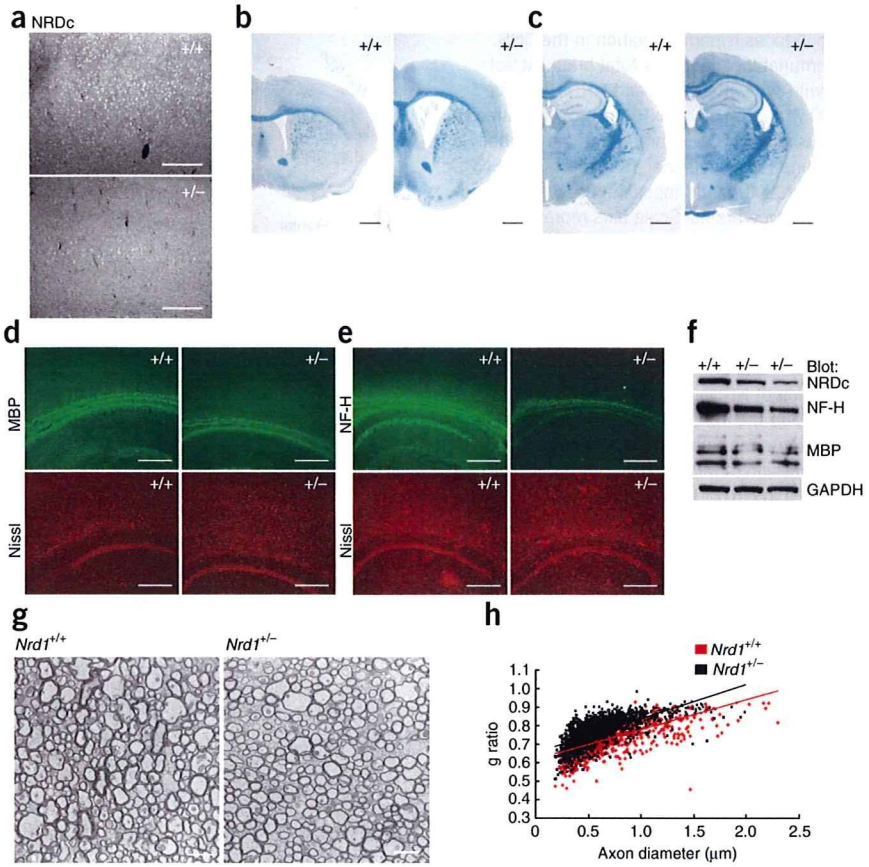

Figure 5 Intermediate CNS phenotype in *Nrd1*$^{+/-}$ mice. (**a**) Immunohistochemistry of *Nrd1*$^{+/-}$ cortex (+/–) with antibody to NRDc showed the obvious reduction of NRDc expression. (**b**,**c**) LFB staining of *Nrd1*$^{+/-}$ brains showed enlarged lateral ventricles, especially in the frontal section (**b**), compared with wild-type brains, but no obvious cortical shrinkage. Scale bars represent 1 mm. (**d**,**e**) Immunohistochemistry of *Nrd1*$^{+/+}$ and *Nrd1*$^{+/-}$ corpus callosum at P90 using antibodies to MBP (**d**) and NF-H (**e**) showed a decrease in the expression of these axonal and myelin markers in *Nrd1*$^{+/-}$ brain. The sections were double-stained with fluorescent Nissl. Scale bars represent 500 μm. (**f**) Immunoblot analysis of whole-brain extracts using antibodies to NRDc, NF-H and MBP. Expression of these proteins was reduced in *Nrd1*$^{+/-}$ brains compared with wild-type littermates. Full-length blots are presented in **Supplementary Figure 9**. (**g**) Electron micrographs of *Nrd1*$^{+/+}$ and *Nrd1*$^{+/-}$ corpus callosum at P120. Scale bars represent 2 μm. (**h**) Scatter plots of g ratio against axon diameters of *Nrd1*$^{+/+}$ and *Nrd1*$^{+/-}$ corpus callosum at P120.

overexpression, we divided mouse brains into two regions: cerebral cortex plus hippocampus (frontal region) and brain stem plus cerebellum (posterior region). Using western blot, we found increased expression of NRDc protein only in the frontal region (**Fig. 6d**). The expression of the myelin markers MBP and CNP was also increased in the frontal region, but not in the posterior region (**Fig. 6d**). We detected higher expression of MBP in corpus callosum by immunostaining (**Fig. 6e**). Notably, analysis of myelination in the NRDc-Tg corpus callosum by electron microscopy revealed that the average g ratio was significantly lower than in wild type, indicating that the myelin sheaths were thicker in NRDc-Tg mice than in wild types (**Fig. 6f–h**). On the other hand, there was no significant difference in the diameter of myelinated axons in the corpus callosum between the NRDc-Tg and wild-type mice (average diameter: wild type, 0.80 ± 0.39 μm; NRDc-Tg, 0.81 ± 0.39 μm, $P = 0.654$). These results provide further evidence that the level of neuronal NRDc regulates myelin sheath thickness. The *Camk2a* promoter is activated around P5, which is after the differentiation of neuronal cells and before subcortical myelination[27]. Thus, NRDc probably affects myelination by regulating axonal signals transmitted from differentiated neurons.

Impaired motor activity and cognitive deficits in *Nrd1*$^{-/-}$ mice

To examine the effect of NRDc on neurological functions, we analyzed *Nrd1*$^{-/-}$ mice with a battery of behavioral tests[28]. We examined neuromuscular strength with grip strength and wire-hanging tests. Although *Nrd1*$^{-/-}$ mice had reduced grip strength (**Fig. 7a**), we found no difference between *Nrd1*$^{+/+}$ and *Nrd1*$^{-/-}$ mice in the wire-hanging test (**Supplementary Fig. 7**), indicating that *Nrd1*$^{-/-}$ mice possess sufficient grip strength to hold their body weight. We next assessed motor coordination and balance with the beam test and rotarod test[29]. In the beam test, *Nrd1*$^{-/-}$ mice moved much slower and slipped more frequently than *Nrd1*$^{+/+}$ mice (**Fig. 7b**,**c**). *Nrd1*$^{-/-}$ mice also had a shorter latency to fall in the rotarod test (**Fig. 7d**). These results indicate that there is a severe impairment of motor coordination and balance in the *Nrd1*$^{-/-}$ mice.

In contrast with motor activity, sensory pathways were apparently conserved in *Nrd1*$^{-/-}$ mice, as their reactions were similar to those of *Nrd1*$^{+/+}$ mice in the hot-plate test (**Supplementary Fig. 7**). We examined cognitive functions of *Nrd1*$^{-/-}$ mice with the T-maze test, in which working memory and reference memory are evaluated by a forced-alternation task and a left right–discrimination task, respectively[30]. In both tasks, *Nrd1*$^{-/-}$ mice took much longer to complete a session, probably as a result of impaired motor activity (**Supplementary Fig. 7** and data not shown). Although the percentage of correct choices in the forced-alternation task was lower in *Nrd1*$^{-/-}$ mice, there were no differences in the left right–discrimination task between *Nrd1*$^{+/+}$ and *Nrd1*$^{-/-}$ mice (**Fig. 7e**,**f**). Together, these results suggest that reference memory is preserved, whereas working memory is impaired in *Nrd1*$^{-/-}$ mice. Although these behavioral alterations are consistent with the axonal and myelination defects, spinal or cerebellar defects might also influence the overall performance of *Nrd1*$^{-/-}$ mice.

NRDc regulates NRG1 shedding through BACE1 and TACE

NRG1, one of the master regulators of myelination, is synthesized as a transmembrane protein and then proteolytically shed from the cell surface[8,10]. Recent reports of hypomyelination in *Bace1*$^{-/-}$ mice have implicated BACE1 in NRG1 shedding[13–15]. NRG1 is also shed from the cell surface by TACE[11], although there is no information about nervous system phenotypes of TACE-deficient mice as a result of their early lethality. These findings, along with the potentiating effect of NRDc on protein ectodomain shedding[19–21], prompted us to examine whether NRDc affects axonal maturation and myelination via regulation of NRG1 shedding by BACE1 or TACE. To determine whether NRDc potentiates BACE1/TACE activity, we carried out transfection experiments in COS7 cells. NRG1 type I was tagged with hemagglutinin (HA) at the

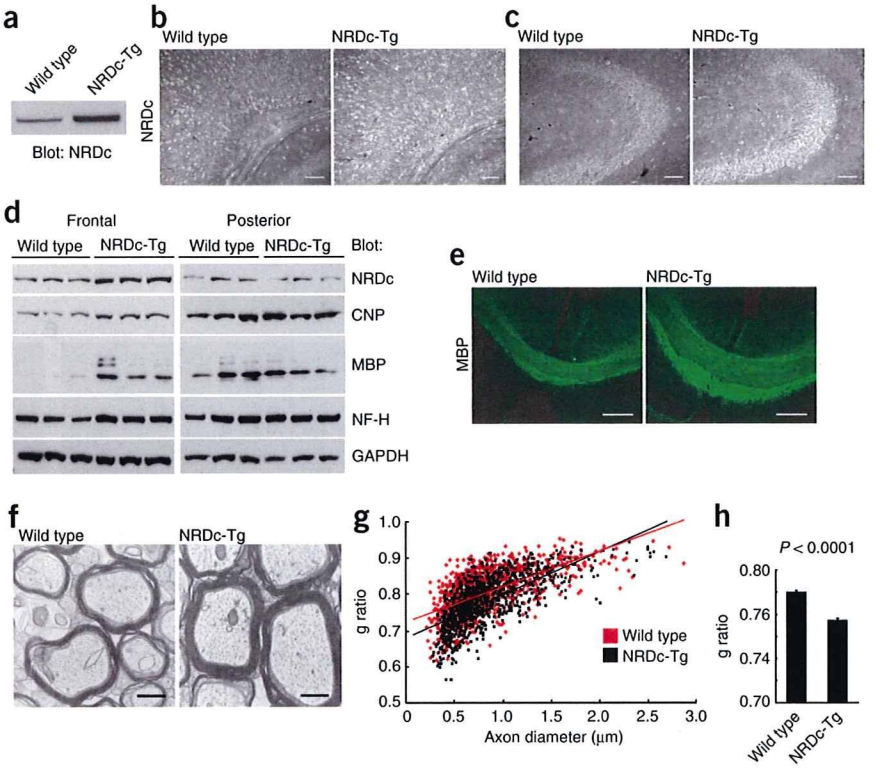

Figure 6 Transgenic overexpression of neuronal NRDc induces hypermyelination in the CNS. (**a**) Immunoblot analysis of total brain extracts from wild-type littermates and NRDc-Tg mice at P90 with antibody to NRDc. (**b**,**c**) We stained sections from NRDc-Tg brains with an antibody to NRDc and found neuronal overexpression of NRDc in the cortex (**b**) and hippocampus (**c**) compared with wild-type brains. Scale bars represent 250 μm. (**d**) Brains of wild-type and NRDc-Tg mice were divided into two regions at the border of cerebral cortex and cerebellum. We analyzed total brain extracts from frontal region and posterior region by immunoblot using antibodies to NRDc, CNP, MBP and NF-H. Note that the increased expression of NRDc, CNP and MBP were only detected in the frontal region. Full-length blots are presented in **Supplementary Figure 9**. (**e**) Expression of MBP in the corpus callosum was increased in NRDc-Tg compared with wild type mice. Scale bars represent 500 μm. (**f**) Electron micrographs of corpus callosum from NRDc-Tg and wild type mice at P30. Scale bars represent 500 nm. (**g**,**h**) Myelin sheaths were thicker in NRDc-Tg mice than in wild types. Scatter plots of g ratios against axon diameters at P30 in NRDc-Tg and wild-type corpus callosum (**g**) and the average g ratio (**h**) are shown. Data represent the mean ± s.e.m. for no fewer than 1,000 myelinated fibers from each group ($n = 4$ for each genotype).

N terminus so that the full length and N-terminal fragment (NTF) of NRG1 type I could be detected with an antibody to HA. Coexpression of NRDc and BACE1 increased NTF levels in total cell lysates, but not in the culture medium (**Fig. 8a**,**b**). In contrast, coexpression of NRDc with TACE clearly increased NTF levels in the culture medium (**Fig. 8a**,**b**). These results suggest that NRDc potentiates TACE-mediated NRG1 cleavage at the cell surface, whereas NRDc enhances BACE1 cleavage of NRG1 in intracellular compartments. Because the enhancement of BACE1-mediated cleavage of NRG1 was not associated with an increase in NTF levels in the culture medium, NRDc is thought to potentiate BACE1 in endocytic pathways and direct the cleaved NRG1 to degradation[31]. Similar to the direct interaction of NRDc and TACE[19], co-precipitation demonstrated that NRDc forms as trimolecular complex with BACE1 and NRG1, suggesting that these proteins physically and functionally interact (**Fig. 8c**).

Given these findings, we examined the expression pattern of endogenous NRG1 protein in fibroblasts derived from *Nrd1*$^{-/-}$ and *Nrd1*$^{+/+}$ mice. Western blot analysis using an antibody to the C terminus of NRG1 (NRG-C), which recognizes both full-length NRG1 and the C-terminal fragment of NRG1 (CTF), revealed an increase in full-length NRG1 and a decrease in CTF in *Nrd1*$^{-/-}$ cells compared with *Nrd1*$^{+/+}$ cells (**Fig. 8d**). In addition, although an antibody to the intracellular N terminus of NRG1 type III detected the cleaved NTF of NRG1 type III in *Nrd1*$^{+/+}$ cells, it barely detected the cleaved fragment in *Nrd1*$^{-/-}$ cells (**Fig. 8d**). These results indicate that NRDc positively regulates the proteolytic cleavage of both type I and type III NRG1.

Next, we examined the expression of NRG1 in brain extracts from *Nrd1*$^{+/+}$ and *Nrd1*$^{-/-}$ mice at P14. Western blotting with antibodies to the C terminus of NRG1 type I and the N terminus of NRG1 type III revealed a similar pattern as found in MEFs (**Fig. 8e**), although the difference between the two genotypes was less evident in the brain extract. These results are consistent with the fact that the proteolytic cleavage of NRG1 type I and type III in brain is regulated by NRDc. We then analyzed the protein expression of BACE1. The molecular

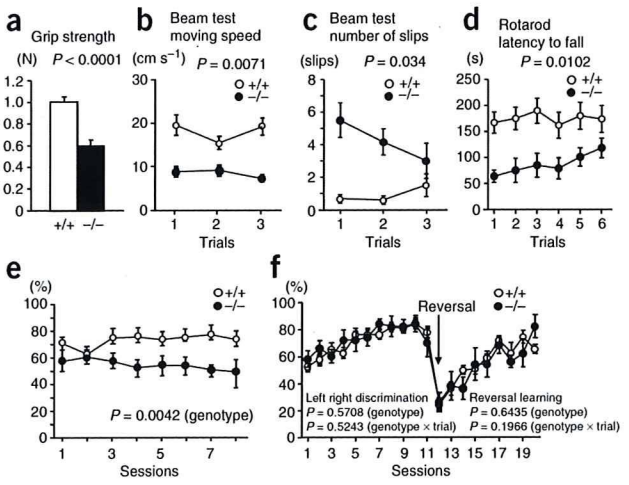

Figure 7 Impaired motor activity and cognitive deficits in *Nrd1*$^{-/-}$ mice. Mice at the age of 90–180 d were analyzed with a battery of behavioral tests (age-matched littermates; *Nrd1*$^{+/+}$, $n = 12$; *Nrd1*$^{-/-}$, $n = 6$). (**a**) Grip-strength test, measured in newtons. *Nrd1*$^{-/-}$ mice had reduced forelimb grip strength. (**b**,**c**) The ability of mice to traverse a narrow beam to reach a dark box was analyzed in a beam test. *Nrd1*$^{-/-}$ mice moved slower (**b**) and slipped more frequently (**c**) than *Nrd1*$^{+/+}$ mice. (**d**) Latency to fall from a rotating drum was measured in a rotarod test. *Nrd1*$^{-/-}$ mice had a shorter latency to fall. (**e**) The percentages of correct choices in the T maze forced-alteration task are shown. showing *Nrd1*$^{-/-}$ mice had impaired working memory. (**f**) The percentages of correct choices in the T maze left right–discrimination task are shown. There was no difference between *Nrd1*$^{+/+}$ and *Nrd1*$^{-/-}$ mice. The genotype effect was analyzed by a two-way repeated ANOVA in all tests. Data represent the mean ± s.e.m.

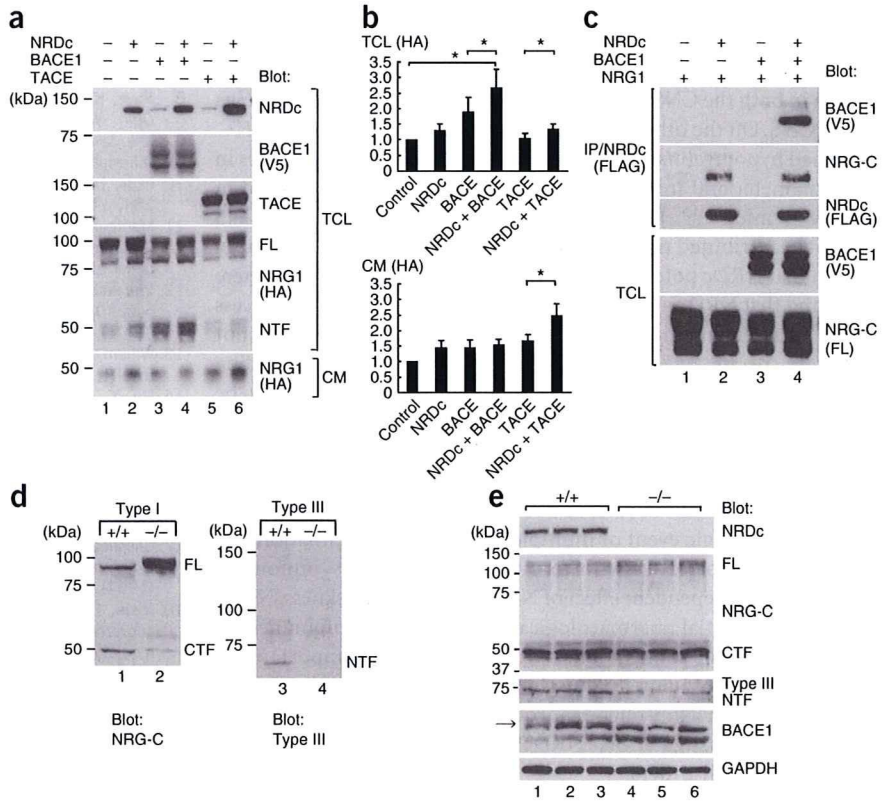

Figure 8 NRDc regulates NRG1 shedding through BACE1 and TACE. (**a**) FLAG-tagged NRDc, V5-tagged BACE1, TACE and HA-tagged NRG1 type1 were coexpressed in COS7 cells. Immunoblot analyses with the indicated antibodies were performed. Note that the cleaved NTF of NRG1 in the total cell lysates (TCL) was increased by the addition of NRDc to BACE1 (lanes 3 and 4), whereas coexpression of NRDc with TACE clearly increased the NTF in the culture medium (CM) (lanes 5 and 6). (**b**) Quantification of the cleaved NTF in the TCL and culture medium by densitometry. The ratio was arbitrarily set at 1 in control vector–transfected cells. Data represent the mean ± s.e.m. in five independent experiments. * $P < 0.05$. (**c**) Immunoprecipitation of the co-transfected cell lysate with an antibody to FLAG reveled a complex of NRDc, BACE1 and NRG1. Only the full length (FL) of NRG1 is shown here. (**d**) Expression of endogenous NRG1 type I and NRG1 type III in MEFs isolated from *Nrd1*$^{+/+}$ or *Nrd1*$^{-/-}$ mice. Note that the full-length of NRG1 type I was increased and the cleaved CTF was decreased in *Nrd1*$^{-/-}$ cells (lane 2) and that the cleaved NTF of NRG1 type III was decreased in *Nrd1*$^{-/-}$ cells (lane 4). (**e**) Immunoblot analysis of brain extracts from control wild-type (+/+) and *Nrd1*$^{-/-}$ (–/–) mice at P14 ($n = 3$ in each genotype) with indicated antibodies. Note that the full length of NRG1 (~140 kDa) was increased, whereas the NTF of NRG1 type III (75 kDa) was decreased in *Nrd1*$^{-/-}$ brains. The mature form of BACE1 in *Nrd1*$^{+/+}$ brain extracts is indicated by an arrow. The ratio of the mature form to immature form was higher in *Nrd1*$^{+/+}$ than in *Nrd1*$^{-/-}$ brains.

size of mature BACE1 in *Nrd1*$^{-/-}$ brain was a little smaller than that in the *Nrd1*$^{+/+}$ brain (**Fig. 8e**). In addition, the ratio of the mature form to immature form of BACE1 was clearly higher in *Nrd1*$^{+/+}$ brains than in *Nrd1*$^{-/-}$ brains (*Nrd1*$^{+/+}$, 2.21 ± 0.62; *Nrd1*$^{-/-}$, 0.75 ± 0.08; $n = 3$, $P = 0.04$), indicating that the protein maturation of BACE1 was impaired in *Nrd1*$^{-/-}$ brains. These results suggest that NRDc regulates BACE1-mediated NRG1 shedding by affecting BACE1 maturation and BACE1 sheddase activity. On the other hand, the mRNA levels of *Nrg1* and *Bace1* were not different between *Nrd1*$^{+/+}$ and *Nrd1*$^{-/-}$ brains (**Supplementary Fig. 8**), indicating that NRDc post-translationally modulates the expression and activity of NRG1 and BACE1.

DISCUSSION

Our findings provide, to the best of our knowledge, the first *in vivo* evidence that NRDc is a critical regulator of axonal maturation and myelination in the CNS and PNS. In the CNS, axon diameter and myelin thickness correlated with levels of NRDc expression (homozygous < heterozygous < wild-type mice). Our results suggest that NRDc affects myelination by regulating axonal maturation, as myelin thickness is proportional to the diameter of axons[1,2]. Neuron-specific overexpression of NRDc, however, did not affect the axon caliber, but instead induced hypermyelination, providing additional evidence that NRDc is a critical regulator of myelination. Notably, as we did not see any differences in the number of oligodendrocyte precursor cells and the expression levels of specific oligodendrocyte precursor markers between *Nrd1*$^{+/+}$ and *Nrd1*$^{-/-}$ mice, NRDc appears to specifically regulate myelination and not oligodendrocyte differentiation or proliferation. In addition, as expression of NRDc is confined to neurons, the effect of NRDc on oligodendrocyte is non–cell autonomous. Instead, our data suggest that NRDc affects axonal signaling between neurons and oligodendrocytes.

NRG1 is the best-characterized neuronal factor that induces axonal signaling required for the entire program of glial differentiation, proliferation and myelination[8,10,32]. NRG1 is synthesized as a transmembrane protein that is proteolytically cleaved in the juxtamembrane region. ADAM proteases (TACE/ADAM17 (ref. 11) and ADAM19 (refs. 12,33)) and BACE1 (refs. 13,14) have been proposed to cleave NRG1. Furthermore, *Bace1*$^{-/-}$ mice exhibit hypomyelination[13–15] and *Adam19*$^{-/-}$ mice have delayed remyelination after injury[33], suggesting that proteolytic cleavage of NRG1 is important for myelination. Our data indicate that NRDc is a critical regulator of NRG1 cleavage *in vivo*. First, the results of our gain-of-function experiments indicate that NRDc enhances BACE1- and TACE-mediated NRG1 cleavage. Second, loss of function in cells resulted in an increase of the full-length NRG1 and a decrease of cleaved NRG1, indicating that NRG1 cleavage is reduced in the absence of NRDc. Third, similar to the results from *Nrd1*$^{-/-}$ cells, we found a decrease of cleaved NRG1 in brain lysates of *Nrd1*$^{-/-}$ mice. *Nrd1*$^{-/-}$ mice also showed hypomyelination in both the CNS and PNS, where NRG1 is a master regulator of myelination. Finally, we found that NRDc formed a complex with BACE1 and NRG1, suggesting that these molecules interact functionally. These results suggest that regulation of NRG1 proteolysis by NRDc is a critical post-translational modification for myelination.

Although several studies have suggested that NRG1 is involved in oligodendrocyte differentiation and CNS myelination[25,32,34], the role of NRG1 in CNS myelination is still controversial as a result of the embryonic lethality of *Nrg1*$^{-/-}$ mice. However, a recent study found normal myelination in a series of conditional null

mutants of *Nrg1* that lack the gene at different stages during CNS development, suggesting that NRG1 may function differently in the PNS and CNS[35]. Because our data indicate that NRDc regulates myelination in both the CNS and PNS, NRDc may affect different proteins in the CNS. On the other hand, although both *Nrd1*$^{-/-}$ and *Bace1*$^{-/-}$ mice had hypomyelination in the CNS and PNS, no abnormalities in axon diameter and initiation of myelination have been reported in *BACE1*$^{-/-}$ mice[13–15]. Taken together, the effect of NRDc in the CNS cannot be attributed merely to NRG1 or BACE1. We have previously shown that NRDc potentiates several ADAM proteases[19–21] and here we found that NRDc also enhanced the capacity of BACE1 to process NRG1. The enhancing effect of NRDc on ADAM proteases is not substrate-specific, as NRDc can potentiate TACE-mediated shedding of HB-EGF, TNF-α, APP and NRG1 (refs. 19–21). This might also be the case for BACE1, as we found that NRDc affects the maturation of BACE1 (**Fig. 8**).

Axonal maturation and myelination are essential in nerve conduction and aberrant in various neuropathologies. For example, the primary pathologic event of multiple sclerosis is demyelination and remyelination correlates with recovery from clinical symptoms[36]. Given the dose-dependent effect of NRDc on myelin thickness, NRDc could be a potential pharmacological target of this common neurological disorder of young adults. NRDc could also be important for the regeneration of injured axons. In fact, the critical regulatory functions of NRDc in axon-oligodendrocyte signaling, axon maturation and myelination suggest that NRDc may impinge on a broad range of neurological disorders.

METHODS

Methods and any associated references are available in the online version of the paper at http://www.nature.com/natureneuroscience/.

Note: Supplementary information is available on the Nature Neuroscience website.

ACKNOWLEDGMENTS

We are grateful to N. Nishimoto and H. Nakabayashi for technical assistance, and K. Matsumoto, E. Kimura, A. Kinoshita and A. Sehara for materials. We thank P.W. Park, T. Nishio, H. Fujiwara, T. Kaneko, F. Fujiyama and H. Kawasaki for critical reading of the manuscript. This study was supported by research grants (19041035, 20390255, 20659061, 20200068 and IBR-shien) from the Ministry of Education, Culture, Sports, Science and Technology of Japan. It was also supported by the Takeda Science Foundation, the Mochida Memorial Foundation for Medical and Pharmaceutical Research, the Suzuken Memorial Foundation, the Japan Health Foundation and the Daiichi Sankyo Sponsored Research Program.

AUTHOR CONTRIBUTIONS

M.O. and E.N. planned the experiments and wrote the manuscript. M.O., Y.H., T.M. and E.N. performed the experiments. H.T. carried out the histological procedures. K.T. and T.M. performed behavioral analysis. N.O. and H.K. generated the *Nrd1*$^{-/-}$ mice. T. Kimura and T. Kita supervised the work.

Published online at http://www.nature.com/natureneuroscience/.
Reprints and permissions information is available online at http://www.nature.com/reprintsandpermissions/.

1. Nave, K.A. & Trapp, B.D. Axon-glial signaling and the glial support of axon function. *Annu. Rev. Neurosci.* **31**, 535–561 (2008).
2. Simons, M. & Trotter, J. Wrapping it up: the cell biology of myelination. *Curr. Opin. Neurobiol.* **17**, 533–540 (2007).
3. Hartline, D.K. & Colman, D.R. Rapid conduction and the evolution of giant axons and myelinated fibers. *Curr. Biol.* **17**, R29–R35 (2007).
4. McTigue, D.M. & Tripathi, R.B. The life, death, and replacement of oligodendrocytes in the adult CNS. *J. Neurochem.* **107**, 1–19 (2008).
5. Griffiths, I. *et al.* Axonal swellings and degeneration in mice lacking the major proteolipid of myelin. *Science* **280**, 1610–1613 (1998).
6. Lappe-Siefke, C. *et al.* Disruption of Cnp1 uncouples oligodendroglial functions in axonal support and myelination. *Nat. Genet.* **33**, 366–374 (2003).
7. Michailov, G.V. *et al.* Axonal neuregulin-1 regulates myelin sheath thickness. *Science* **304**, 700–703 (2004).
8. Nave, K.A. & Salzer, J.L. Axonal regulation of myelination by neuregulin 1. *Curr. Opin. Neurobiol.* **16**, 492–500 (2006).
9. Mei, L. & Xiong, W.C. Neuregulin 1 in neural development, synaptic plasticity and schizophrenia. *Nat. Rev. Neurosci.* **9**, 437–452 (2008).
10. Falls, D.L. Neuregulins: functions, forms and signaling strategies. *Exp. Cell Res.* **284**, 14–30 (2003).
11. Montero, J.C., Yuste, L., Diaz-Rodriguez, E., Esparis-Ogando, A. & Pandiella, A. Differential shedding of transmembrane neuregulin isoforms by the tumor necrosis factor alpha-converting enzyme. *Mol. Cell. Neurosci.* **16**, 631–648 (2000).
12. Shirakabe, K., Wakatsuki, S., Kurisaki, T. & Fujisawa-Sehara, A. Roles of Meltrin beta/ADAM19 in the processing of neuregulin. *J. Biol. Chem.* **276**, 9352–9358 (2001).
13. Willem, M. *et al.* Control of peripheral nerve myelination by the beta-secretase BACE1. *Science* **314**, 664–666 (2006).
14. Hu, X. *et al.* Bace1 modulates myelination in the central and peripheral nervous system. *Nat. Neurosci.* **9**, 1520–1525 (2006).
15. Hu, X. *et al.* Genetic deletion of BACE1 in mice affects remyelination of sciatic nerves. *FASEB J.* **22**, 2970–2980 (2008).
16. Pierotti, A.R. *et al.* N-arginine dibasic convertase, a metalloendopeptidase as a prototype of a class of processing enzymes. *Proc. Natl. Acad. Sci. USA* **91**, 6078–6082 (1994).
17. Chesneau, V. *et al.* N-arginine dibasic convertase (NRD convertase): a newcomer to the family of processing endopeptidases. An overview. *Biochimie* **76**, 234–240 (1994).
18. Nishi, E., Prat, A., Hospital, V., Elenius, K. & Klagsbrun, M. N-arginine dibasic convertase is a specific receptor for heparin-binding EGF-like growth factor that mediates cell migration. *EMBO J.* **20**, 3342–3350 (2001).
19. Nishi, E., Hiraoka, Y., Yoshida, K., Okawa, K. & Kita, T. Nardilysin enhances ectodomain shedding of heparin-binding epidermal growth factor-like growth factor through activation of tumor necrosis factor alpha-converting enzyme. *J. Biol. Chem.* **281**, 31164–31172 (2006).
20. Hiraoka, Y. *et al.* Enhancement of alpha-secretase cleavage of amyloid precursor protein by a metalloendopeptidase nardilysin. *J. Neurochem.* **102**, 1595–1605 (2007).
21. Hiraoka, Y. *et al.* Ectodomain shedding of TNF-alpha is enhanced by nardilysin via activation of ADAM proteases. *Biochem. Biophys. Res. Commun.* **370**, 154–158 (2008).
22. Bernstein, H.G. *et al.* Histochemical evidence for wide expression of the metalloendopeptidase nardilysin in human brain neurons. *Neuroscience* **146**, 1513–1523 (2007).
23. Lu, Q.R. *et al.* Common developmental requirement for Olig function indicates a motor neuron/oligodendrocyte connection. *Cell* **109**, 75–86 (2002).
24. Fields, R.D. & Ellisman, M.H. Axons regenerated through silicone tube splices. II. Functional morphology. *Exp. Neurol.* **92**, 61–74 (1986).
25. Taveggia, C. *et al.* Neuregulin-1 type III determines the ensheathment fate of axons. *Neuron* **47**, 681–694 (2005).
26. Mayford, M., Wang, J., Kandel, E.R. & O'Dell, T.J. CaMKII regulates the frequency-response function of hippocampal synapses for the production of both LTD and LTP. *Cell* **81**, 891–904 (1995).
27. Dragatsis, I. & Zeitlin, S. CaMKIIalpha-Cre transgene expression and recombination patterns in the mouse brain. *Genesis* **26**, 133–135 (2000).
28. Yamasaki, N. *et al.* Alpha-CaMKII deficiency causes immature dentate gyrus, a novel candidate endophenotype of psychiatric disorders. *Mol Brain* **1**, 6 (2008).
29. Carter, R.J. *et al.* Characterization of progressive motor deficits in mice transgenic for the human Huntington's disease mutation. *J. Neurosci.* **19**, 3248–3257 (1999).
30. Takao, K. *et al.* Impaired long-term memory retention and working memory in sdy mutant mice with a deletion in Dtnbp1, a susceptibility gene for schizophrenia. *Mol Brain* **1**, 11 (2008).
31. Thinakaran, G. & Koo, E.H. Amyloid precursor protein trafficking, processing and function. *J. Biol. Chem.* **283**, 29615–29619 (2008).
32. Calaora, V. *et al.* Neuregulin signaling regulates neural precursor growth and the generation of oligodendrocytes *in vitro*. *J. Neurosci.* **21**, 4740–4751 (2001).
33. Wakatsuki, S., Yumoto, N., Komatsu, K., Araki, T. & Sehara-Fujisawa, A. Roles of meltrin-beta/ADAM19 in progression of Schwann cell differentiation and myelination during sciatic nerve regeneration. *J. Biol. Chem.* **284**, 2957–2966 (2009).
34. Taveggia, C. *et al.* Type III neuregulin-1 promotes oligodendrocyte myelination. *Glia* **56**, 284–293 (2008).
35. Brinkmann, B.G. *et al.* Neuregulin-1/ErbB signaling serves distinct functions in myelination of the peripheral and central nervous system. *Neuron* **59**, 581–595 (2008).
36. Trapp, B.D. & Nave, K.A. Multiple sclerosis: an immune or neurodegenerative disorder? *Annu. Rev. Neurosci.* **31**, 247–269 (2008).

Cardiovasc Interv and Ther (2010) 25:29–39
DOI 10.1007/s12928-009-0005-4

ORIGINAL ARTICLE

Incidence and outcome of surgical procedures after sirolimus-eluting stent implantation: a report from the j-Cypher registry

Takeshi Kimura · Takaaki Isshiki · Yasuhiko Hayashi · Shigeru Oshima · Masanobu Namura · Hitoshi Nakashima · Kazuya Kawai · Takahito Sone · Ryozo Tatami · Taiichiro Meguro · Masakiyo Nobuyoshi · Kazuaki Mitsudo

Received: 6 October 2009 / Accepted: 9 October 2009 / Published online: 13 November 2009

Abstract The incidence of surgical procedures after sirolimus-eluting stent (SES) implantation and, more importantly, the rate of perioperative stent thrombosis (ST) and/or other adverse events have not yet been adequately addressed. The incidence and outcome of the surgical procedures after SES implantation were prospectively evaluated in a large-scale multicenter registry of patients undergoing SES implantation. Among 12,824 patients enrolled in the registry, cumulative incidences of surgical procedures were 0.7% at 60 days, 5.1% at 1 year and 14.7% at 3 years. Surgical procedures were performed in 1,430 patients including non-coronary artery bypass graft (CABG) surgery in 1,275 patients and CABG in 189 patients. The incidences of death/myocardial infarction/ST (definite or probable) and ST (definite or probable) at 30 days after surgical procedures were 2.7 and 0.35%, respectively. Surgery performed within 60 days after SES implantation as compared with that performed beyond 60 days was associated with significantly higher incidences of death/myocardial infarction/ST (definite or probable) and ST (definite or probable) at 30 days after surgical procedures (6.4 vs. 2.5%: $P = 0.02$ and 2.2 vs. 0.23%: $P = 0.002$, respectively). Surgery within 60 days as well as hemodialysis and small body mass index were independent risk factors of death/myocardial infarction/ST (definite or probable) identified by multivariable analysis. Surgical procedures were required fairly often after SES implantation. The incidences of adverse cardiac events including ST after surgical procedures were acceptably low. Surgery within 60 days after SES implantation carried significantly higher risks as compared with those beyond 60 days.

On behalf of the j-Cypher Registry investigators.

T. Kimura (✉)
Department of Cardiovascular of Medicine,
Graduate School of Medicine, Kyoto University,
54 Shogoin Kawahara-cho, Sakyo-ku, Kyoto 606-8507, Japan
e-mail: taketaka@kuhp.kyoto-u.ac.jp

T. Isshiki
Teikyo University Hospital, Tokyo, Japan

Y. Hayashi
Tsuchiya General Hospital, Hiroshima, Japan

S. Oshima
Gunma Prefectural Cardiovascular Center, Gunma, Japan

M. Namura
Kanazawa Cardiovascular Hospital, Kanazawa, Japan

H. Nakashima
National Hospital Organization Kagoshima Medical Center,
Kagoshima, Japan

K. Kawai
Chikamori Hospital, Kochi, Japan

T. Sone
Ogaki Municipal Hospital, Ogaki, Japan

R. Tatami
Maizuru Kyosai Hospital, Maizuru, Japan

T. Meguro
Sendai Health Hospital, Sendai, Japan

M. Nobuyoshi
Kokura Memorial Hospital, Kokura, Japan

K. Mitsudo
Kurashiki Central Hospital, Kurashiki, Japan

Keywords Stent · Thrombosis · Revascularization · Surgery · Aspirin

Introduction

Non-cardiac surgical procedures after bare-metal stent (BMS) implantation have been reported to be associated with a high rate of perioperative stent thrombosis (ST) and/or serious adverse events in the first 6 weeks after stent implantation [1–4]. When surgical procedures were performed beyond 6–8 weeks after BMS implantation, the risk of perioperative ST was reported to attenuate markedly [1, 2, 4]. In the era of the drug-eluting stent (DES), a report of three cases with postoperative ST late (343–442 days) after DES implantation highlighted the exaggerated ST risk after surgical procedures [5]. Pressed by this and other reports suggesting safety concerns related to DES [6–8], a consensus statement from the American College of Cardiology and the American Heart Association recommended postponing elective surgery for at least 1 year in patients in whom a DES had been implanted [9]. However, the incidence of surgical procedures after DES implantation and more importantly the rates of perioperative ST and/or serious adverse events have not yet been systematically evaluated [10]. Furthermore, although perioperative management of antiplatelet therapy (APT) is an issue discussed frequently in clinical practice, optimal perioperative management of patients with prior DES implantation has not yet been adequately defined. To address these issues, the incidence and outcome of the surgical procedures after percutaneous coronary intervention (PCI) using DES were prospectively evaluated in a large-scale multicenter registry of patients undergoing sirolimus-eluting stent (SES) implantation.

Methods

Study population

The j-CYPHER registry is a physician-initiated prospective multicenter observational study in Japan enrolling consecutive patients undergoing SES implantation. The study design and the 2-year outcome were reported previously [11]. Between August 2004 and November 2006, 12,824 patients with 19,675 lesions were enrolled in the registry.

Surgical procedures during follow-up including CABG were captured as follow-up events. Percutaneous endovascular procedures were not regarded as surgical procedures. Gastrointestinal endoscopic therapeutic procedures were included in the surgical procedures. Although the data on the type of the surgical procedures were reported, we did not collect detailed information on the surgical procedures such as the type of anesthesia, urgency of the surgical procedures and periprocedural bleeding complications. The timing of the surgical procedures after SES implantation was categorized into the two groups (within 60 days and beyond 60 days after SES implantation) based on the previous reports suggesting increased risk of severe adverse events in patients undergoing surgical procedures within 6–8 weeks after BMS implantation [1–4].

Status on APT for both aspirin and thienopyridine was also prospectively recorded. The recommended APT regimen was aspirin (≥81 mg daily) indefinitely and thienopyridine (200 mg ticlopidine or 75 mg clopidogrel daily) for at least 3 months after SES implantation. The duration of dual APT and management of perioperative APT was left to the discretion of each attending physician. Status of APT at the time of the surgical procedures was categorized into four groups (dual, aspirin alone, thienopyridine alone and none). Information regarding periprocedural bridging use of heparin and/or other short-acting antiplatelet agents was not systematically collected.

Follow-up data were obtained from hospital charts or by contacting patients and/or referring physicians at 30 days, 6 months, 1, 2 and 3 years. Complete 1-year follow-up was achieved in 97% of patients; median duration of follow-up was 883 days (interquartile range 632–1,095 days) for survival status and 820 days (interquartile range 502–1,095 days) for surgical procedures. The relevant review boards in all 37 participating centers approved the study protocol (Supplementary Appendix). Written informed consent for participation in the study was obtained from all patients.

Outcomes and definitions

The primary outcome measure for the current analysis was the time, until 30 days after the surgical procedures, to the first occurrence of composite of death, myocardial infarction (MI) and/or ST (definite or probable). Individual components of the primary outcome measure as well as definite ST within 30 days after the surgical procedures were also evaluated.

Death was regarded as cardiac in origin unless obvious non-cardiac causes could be identified. Sudden death was defined as unexplained death in previously stable patients. MI was adjudicated according to the definition in the Arterial Revascularization Therapy Study [12]. Measurement of cardiac biomarkers such as troponin or creatinine phosphokinase was not performed routinely after the surgical procedures, but was generally performed only when periprocedural MI was clinically suspected. ST was defined according to the Academic Research Consortium (ARC) definition [13]. Both ARC definite and definite/probable ST were evaluated.

Statistical analysis

Baseline characteristics were compared between the patients with surgical procedures and those patients who completed 3-year follow-up without surgical procedures. Baseline characteristics of patients were not evaluated at the time of the surgical procedures, but at the time of the index SES implantation. Categorical variables were compared with the chi-square test. Continuous variables were compared using the Student's *t* test or Wilcoxon rank sum test based on the distribution.

Cumulative incidences of the surgical procedures and the adverse events after the surgical procedures were estimated by the Kaplan–Meier method. Differences in the adverse event rates after the surgical procedures according to the timing of the surgical procedures and the status of perioperative APT were assessed with the log-rank test.

A Cox proportional hazards model was used to identify independent risk factors of the primary outcome measure. We used the variables listed in Table 1 and the timing of the surgical procedures after SES implantation as potential independent variables. The continuous variables were dichotomized by clinically meaningful reference values or median values. To determine the independent risk factors, we selected variables with *P* values less than 0.05 in the univariable Cox models and included them simultaneously

Table 1 Baseline characteristics of patients with or without surgical procedures during 3-year follow-up

Variables	All patients (N = 12,824)	With surgery (N = 1,430)	Without surgery (N = 3,685)	*P* value
Age (years)	68.4 ± 10.3	69.5 ± 9.4	67.3 ± 10.0	<0.0001
Age >70 years	5,925 (46%)	734 (51%)	1,541 (42%)	<0.0001
Male gender	9,653 (75%)	1,087 (76%)	2,794 (76%)	0.88
BMI	23.9 ± 3.4	23.7 ± 3.5	24.1 ± 3.3	<0.0001
BMI ≤25.0	8,384 (65%)	990 (69%)	2,329 (63%)	<0.0001
Emergency procedure for				
ACS	1,925 (15%)	197 (14%)	459 (12%)	0.21
STEMI	1,253 (9.8%)	117 (8.2%)	299 (8.1%)	0.95
Prior heart failure	1,793 (14%)	283 (20%)	373 (10%)	<0.0001
Prior MI	3,488 (27%)	407 (28%)	1,094 (30%)	0.39
Prior stroke	1,218 (9.5%)	175 (12%)	270 (7.3%)	<0.0001
Prior coronary revascularization	6,305 (49%)	724 (51%)	2,016 (55%)	0.009
Peripheral vascular disease	1,524 (12%)	276 (19%)	340 (9.2%)	<0.0001
eGFR	58.6 ± 23.1	53.1 ± 27.2	60.9 ± 21.0	<0.0001
eGFR <30 ml/min/1.73 m^2/				
Non-HD	630 (4.9%)	116 (8.1%)	129 (3.5%)	<0.0001
HD	682 (5.3%)	160 (11%)	113 (3.1%)	<0.0001
Hypertension	9,559 (75%)	1,096 (77%)	2,676 (73%)	0.003
Diabetes	5,320 (41%)	677 (47%)	1,560 (42%)	0.001
Diabetes on insulin therapy	1,205 (9.4%)	182 (13%)	334 (9.1%)	0.0001
Current smoker	2,606 (20%)	282 (20%)	714 (19%)	0.78
Single vessel disease	5,770 (45%)	578 (40%)	1,689 (46%)	0.0005
Target of unprotected LMCA	582 (4.5%)	72 (5.0%)	163 (4.4%)	0.35
Target of LAD	6,984 (54%)	734 (51%)	1,966 (53%)	0.19
LVEF	57.8 ± 13.4	56.2 ± 13.9	58.3 ± 12.7	<0.0001
LVEF ≤ 40%	1,259 (11%)	183 (15%)	311 (9.7%)	<0.0001
Multivessel dilatation	3,568 (28%)	420 (29%)	952 (26%)	0.02
Number of stents per patient	1.93 ± 1.19	2.0 ± 1.23	1.91 ± 1.17	0.02
Number of stents per patient ≥2	6,844 (53%)	775 (54%)	1,950 (53%)	0.39
Total stent length (mm)	42.5 ± 28.3	44.3 ± 30.2	41.2 ± 27.1	<0.0001
Total stent length >36 mm	5,813 (45%)	657 (46%)	1,636 (44%)	0.3

Patients without surgery included only those patients who completed 3-year follow-up without surgical procedures

ACS acute coronary syndrome, *BMI* body mass index, *eGFR* estimated glomerular filtration rate, *HD* hemodialysis, *LAD* left anterior descending coronary artery, *LMCA* left main coronary artery, *LVEF* left ventricular ejection fraction, *STEMI* ST segment elevation myocardial infarction

in the multivariable models. All analyses were conducted by a physician (Takeshi Kimura) with the use of JMP 8 (SAS Institute Inc, Cary, NC), and all reported *P* values were two-sided.

The study sponsor was not involved in the study design, in the collection, analysis and interpretation of data, the writing of the report or the decision to submit the paper for publication.

Results

Incidence of surgical procedures after SES implantation

Patients with high-risk features such as old age, diabetes and renal failure were commonly enrolled in the j-Cypher registry (Table 1). During the 3-year follow-up after PCI using SES, surgical procedures were performed commonly and constantly (annual rate of 5%). Cumulative incidences of surgical procedures were 0.7% at 60 days, 5.1% at 1 year, 10.2% at 2 years and 14.7% at 3 years (Fig. 1). Surgical procedures were performed in 1,430 patients including non-CABG surgery in 1,275 patients and CABG in 189 patients. Common surgical fields for non-CABG surgery included abdominal surgery, vascular surgery, orthopedic surgery, ophthalmic surgery, pacemaker implantation, gastrointestinal endoscopic procedures and urologic surgery (Table 2).

As compared with patients who did not have surgery, patients who had surgery were older and had smaller body mass indexes. Patients who had surgery more often had comorbidities such as heart failure, stroke, peripheral vascular disease, end-stage renal disease, hypertension and diabetes. In terms of extensiveness of coronary artery disease and procedural complexities, patients who had surgery more often had multi-vessel coronary artery disease and low left ventricular ejection fraction, and more often underwent multi-vessel dilatation with longer total stent length. The proportion of patients undergoing emergency procedures for acute coronary syndrome was similar in both groups (Table 1).

Clinical outcome after SES implantation and after surgical procedures

Adverse event rates through 3 years for the entire j-Cypher registry cohort are summarized in Table 3. The slopes of

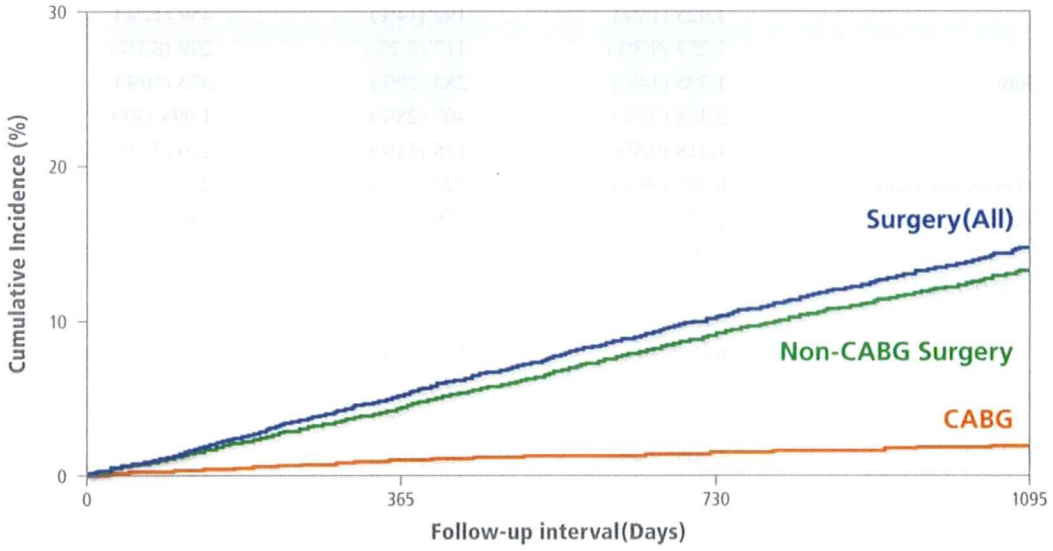

Surgery(All)		60 Days	1 year	2 years	3 years
Incidence		0.7%	5.1%	10.2%	14.7%
Number of events		94	626	1146	1430
Number of patients at risk	12824	12492	11358	8264	3687
Non-CABG Surgery					
Incidence		0.6%	4.3%	9.0%	13.3%
Number of events		75	526	1011	1275
Number of patients at risk	12824	12509	11448	8367	3751
CABG					
Incidence		0.2%	0.9%	1.4%	1.9%
Number of events		20	111	161	189
Number of patients at risk	12824	12559	11814	8984	4149

Fig. 1 Cumulative incidences of surgical procedures after sirolimus-eluting stent implantation. *CABG* coronary artery bypass grafting surgery

the cumulative incidence curves between 30 days and 3 years were 0.3% per month for death/MI/ST (definite or probable), 0.25% per month for death, 0.07% per month for MI, and 0.02% per month for both definite and definite/probable ST. Clinical outcomes after surgical procedures are summarized in Fig. 2 and Table 4. The incidences of death/MI/ST (definite or probable) and ST (definite or probable) at 30 days after surgical procedures were 2.7 and 0.35%, respectively. The cumulative incidence curve for death/MI/ST (definite or probable) revealed increased early risk at 30 days and relatively constant risk beyond 30 days after surgical procedures (Fig. 2a). The slope of the cumulative incidence curve beyond 30 days after surgical procedures was relatively steep (0.67% per month). Stent thrombosis occurred mostly within 30 days after surgical procedures (Fig. 2b). One patient who had ST while stopping APT before the scheduled but aborted surgical procedure was not included in the group with surgical procedures.

Causes of death within 30 days after surgical procedures included cardiac death in 15 patients and non-cardiac death in 18 cases. Stent thrombosis was suspected as the cause of death in only two patients (a probable ST and a sudden cardiac death post CABG) (Table 5).

Table 2 Fields of surgical procedures other than CABG

Surgical fields	Number of patients (%)
All	1,275 (100)
Abdominal surgery	241 (19)
Vascular surgery	224 (18)
Orthopedic surgery	173 (14)
Ophthalmic surgery	161 (13)
Pacemaker implantation	97 (7.6)
Gastrointestinal endoscopic procedures	96 (7.5)
Urologic surgery	76 (6.0)
Cardiac surgery	46 (3.6)
Neurosurgery	32 (2.5)
Respiratory surgery	31 (2.4)
Otorhinolaryngological surgery	29 (2.3)
Dermatologic surgery	21 (1.7)
Oral and maxillofacial surgery	18 (1.4)
Gynecological surgery	9 (0.7)
Mammary surgery	9 (0.7)
Others	10 (0.8)
Unknown	2 (0.2)

CABG coronary artery bypass grafting surgery

Timing of surgical procedures and clinical outcome

Surgery performed within 60 days after SES implantation as compared with that performed beyond 60 days was associated with significantly higher incidences of death/MI/ST (definite or probable) and ST (definite or probable) within 30 days after surgical procedures (6.4 vs. 2.5%: $P = 0.02$ and 2.2 vs. 0.23%: $P = 0.002$, respectively) (Fig. 3, Table 6). Increased risk for surgical procedures performed within 60 days after SES implantation was consistently seen after excluding CABG (Table 6).

Perioperative status of antiplatelet therapy

Antiplatelet therapy before surgery was dual in 400 patients (28%), aspirin alone in 434 patients (30%),

Table 3 Adverse event rates for 3 years after SES implantation in the entire j-Cypher registry cohort

	Cumulative event rate			
	30 days (%)	1 year (%)	2 years (%)	3 years (%)
Death/MI/ST (definite or probable)	1.2	4.9	8.2	11.6
Death	0.74	4.0	6.8	9.5
Cardiac death	0.72	2.4	3.5	4.6
Sudden death	0.08	0.68	1.2	1.6
MI	0.38	1.1	1.7	2.8
Related to stent thrombosis	0.29	0.54	0.74	1.1
Stroke	0.39	1.9	3.2	4.1
Stent thrombosis				
Definite	0.36	0.61	0.84	1.2
Definite/probable	0.48	0.77	1.0	1.3
Definite/probable/possible	0.49	1.5	2.3	3.3
Target lesion revascularization	0.71	9.0	12.0	14.1
Coronary artery bypass grafting	0.11	0.91	1.4	1.9
Any coronary revascularization	2.7	21.6	27.8	32.4

MI myocardial infarction, *SES* sirolimus-eluting stent, *ST* stent thrombosis

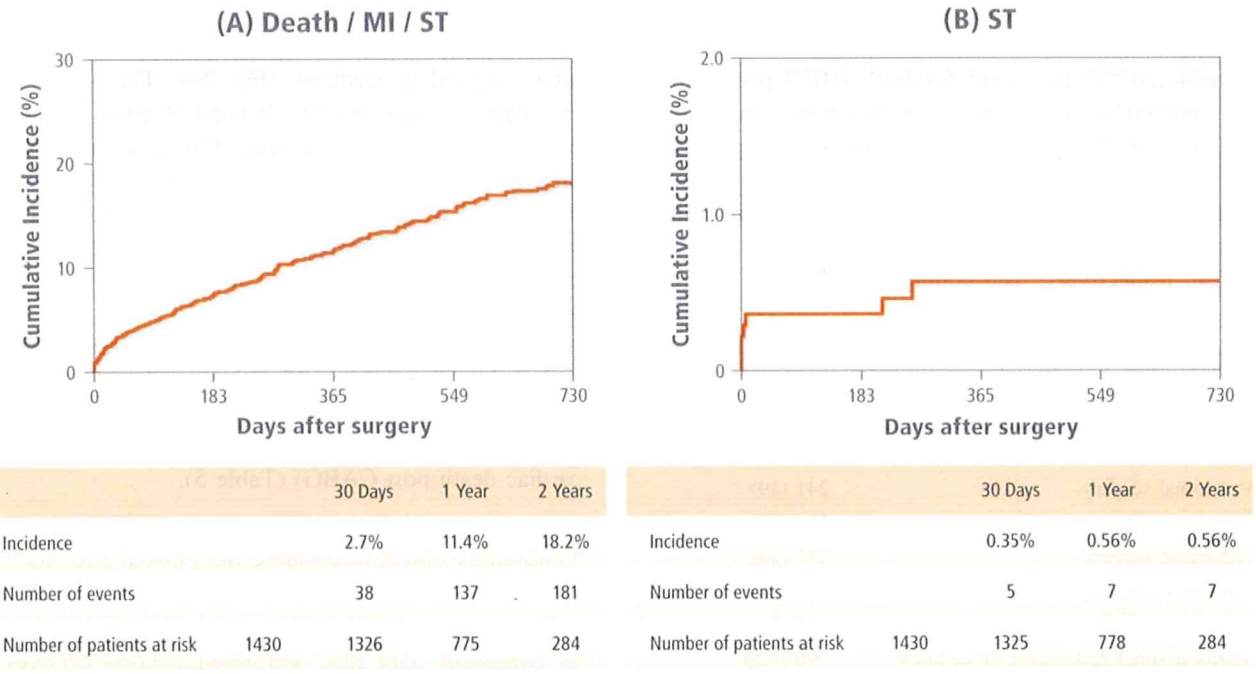

	30 Days	1 Year	2 Years
Incidence	2.7%	11.4%	18.2%
Number of events	38	137	181
Number of patients at risk 1430	1326	775	284

	30 Days	1 Year	2 Years
Incidence	0.35%	0.56%	0.56%
Number of events	5	7	7
Number of patients at risk 1430	1325	778	284

Fig. 2 Cumulative incidences of death/MI/ST (**a**) and ST (**b**) after surgical procedures. *MI* myocardial infarction and *ST* stent thrombosis (definite or probable)

Table 4 Adverse event rates after surgical procedures

Endpoints	*N* of events (incidence)		
	30 days (%)	1 year (%)	2 years (%)
Death/MI/ST (definite or probable)	38 (2.7)	137 (11.4)	181 (18.2)
Death	33 (2.4)	128 (10.7)	171 (17.3)
MI	9 (0.65)	16 (1.3)	18 (1.6)
ST (definite or probable)	5 (0.35)	7 (0.56)	7 (0.56)
ST (definite)	4 (0.28)	6 (0.49)	6 (0.49)

MI myocardial infarction, *ST* stent thrombosis

thienopyridine alone in 19 patients (1.3%) and none in 577 patients (40%). Incidences of death/MI/ST (definite or probable) and ST (definite or probable) at 30 days after surgical procedures were not different according to the perioperative status of APT (Table 7).

Risk factors of perioperative death/MI/ST (definite or probable)

Risk factors of perioperative death/MI/ST (definite or probable) identified by univariate analysis included hemodialysis, small body mass index, prior heart failure and surgery within 60 days after SES implantation. Surgery within 60 days after SES implantation as well as hemodialysis and small body mass index were independent risk factors of perioperative death/MI/ST (definite or probable) identified by multivariable analysis (Table 8).

Table 5 Causes of death within 30 days after surgical procedures

Causes of death	Number of cases
Cardiac death	15
MI, probable ST	1
Sudden cardiac death (post CABG)	1
Postoperative MI, no evidence of ST	3
Heart failure, no evidence of MI	5
Complications of preoperative MI	4
Unknown	1
Non-cardiac death	18
Infection	7
Renal failure	3
Stroke	3
Bleeding	1
Others	4

CABG coronary artery bypass grafting surgery, *MI* myocardial infarction, *ST* stent thrombsis

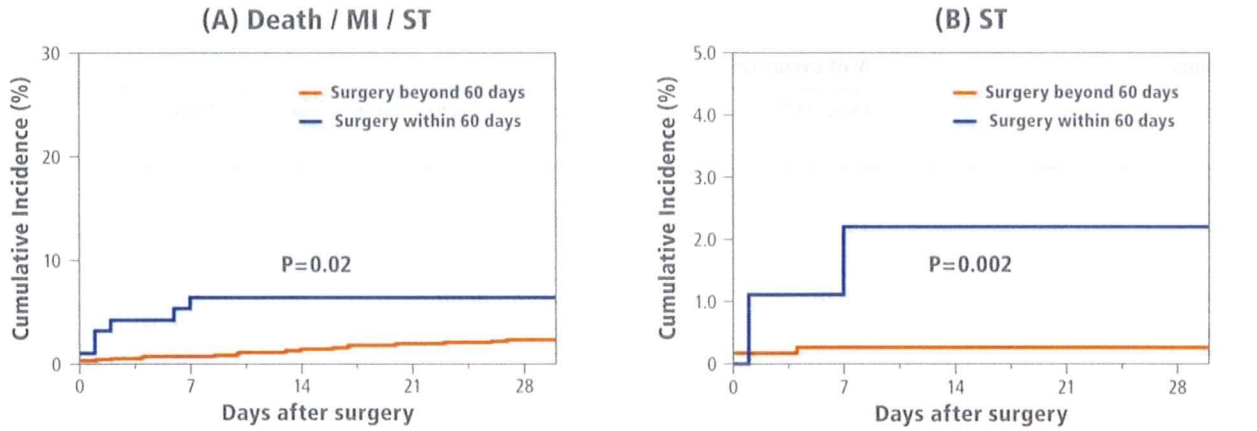

Surgery within 60 days		7 Days	30 Days
Incidence		6.4%	6.4%
Number of events		6	6
Number of patients at risk	94	89	87
Surgery beyond 60 days			
Incidence		0.8%	2.5%
Number of events		10	32
Number of patients at risk	1336	1306	1239

Surgery within 60 days		7 Days	30 Days
Incidence		2.2%	2.2%
Number of events		2	2
Number of patients at risk	94	89	87
Surgery beyond 60 days			
Incidence		0.23%	0.23%
Number of events		3	3
Number of patients at risk	1336	1306	1238

Fig. 3 Cumulative incidences of death/MI/ST (**a**) and ST (**b**) after surgical procedures compared between surgery within and beyond 60 days after sirolimus-eluting stent implantation. *MI* myocardial infarction and *ST* stent thrombosis (definite or probable)

Table 6 Adverse event rates at 30 days after surgical procedures according to the timing after SES implantation

Endpoints	*N* of events (incidence) at 30 days after surgery		
	Surgery within 60 days	Surgery beyond 60 days	*P* value
Surgery (all)	*N* = 94	*N* = 1336	
Death/MI/ST (definite or probable)	6 (6.4%)	32 (2.5%)	0.02
Death	4 (4.3%)	29 (2.2%)	0.17
MI	2 (2.2%)	7 (0.54%)	0.06
ST (definite or probable)	2 (2.2%)	3 (0.23%)	0.002
ST (definite)	2 (2.2%)	2 (0.15%)	0.0004
Non-CABG surgery	*N* = 75	*N* = 1200	
Death/MI/ST (definite or probable)	5 (6.5%)	27 (2.3%)	0.02
Death	3 (3.9%)	24 (2.1%)	0.25
MI	2 (2.7%)	7 (0.6%)	0.03
ST (definite or probable)	2 (2.7%)	3 (0.25%)	0.001
ST (definite)	2 (2.7%)	2 (0.17%)	0.0002

MI myocardial infarction, *SES* sirolimus-eluting stent, *ST* stent thrombosis

Discussion

The main findings of the present study were that surgical procedures were often required after PCI using SES (5% per year) and that the incidences of adverse cardiac events including ST after surgical procedures were acceptably low, although surgery within 60 days after SES implantation carried significantly higher risks as compared with surgery beyond 60 days after SES implantation.

A consensus statement from the American College of Cardiology and the American Heart Association recommended BMS implantation or balloon angioplasty with

Table 7 Adverse event rates at 30 days after surgical procedures according to the status of preoperative antiplatelet therapy

Endpoints	*N* of events (incidence)				
	Dual APT $N = 400$ (%)	Aspirin alone $N = 434$ (%)	Thienopyridine alone $N = 19$ (%)	None $N = 577$ (%)	*P* value
Death/MI/ST (definite or probable)	15 (3.8)	12 (2.9)	0 (0)	11 (1.9)	0.3
Death	15 (3.8)	10 (2.4)	0 (0)	8 (1.4)	0.09
MI	2 (0.53)	3 (0.7)	0 (0)	4 (0.7)	0.96
ST (definite or probable)	0 (0)	2 (0.47)	0 (0)	3 (0.52)	0.55
ST (definite)	0 (0)	2 (0.47)	0 (0)	2 (0.35)	0.62

MI myocardial infarction, *ST* stent thrombosis

Table 8 Univariate and multivariable analysis for risk factors of perioperative death/MI/ST (definite or probable)

Variables	Univariate analysis			Multivariable analysis		
	N of events (incidence)			Odds ratio	95% CI	*P* value
	Yes (%)	No (%)	*P* value			
Age >70 years	19 (2.6)	18 (2.6)	0.98			
Male gender	27 (2.5)	10 (2.9)	0.66			
BMI ≤25.0	32 (3.3)	5 (1.2)	0.02	1.59	1.03–2.73	0.03
Emergency procedure for						
ACS	8 (4.1)	29 (2.4)	0.16			
STEMI	4 (3.6)	33 (2.6)	0.51			
Prior heart failure	13 (4.7)	24 (2.1)	0.02	1.32	0.92–1.86	0.13
Prior MI	12 (3.0)	25 (2.5)	0.57			
Prior stroke	8 (4.6)	29 (2.4)	0.08			
Prior coronary revascularization	16 (2.3)	21 (3.0)	0.36			
Peripheral vascular disease	10 (3.7)	27 (2.4)	0.23			
eGFR <30 ml/min/1.73 m^2/						
Non-HD	5 (4.4)	32 (2.5)	0.22			
HD	11 (6.9)	26 (2.1)	0.003	1.64	1.12–2.34	0.01
Hypertension	28 (2.6)	9 (2.8)	0.86			
Diabetes	12 (1.8)	25 (3.4)	0.06			
Diabetes on insulin therapy	5 (1.2)	32 (2.6)	0.92			
Current smoker	8 (2.9)	29 (2.6)	0.77			
Single vessel disease	12 (2.1)	25 (3.0)	0.33			
Target of unprotected LMCA	0 (0)	37 (2.8)	0.16			
Target of LAD	15 (2.1)	22 (3.2)	0.19			
LVEF ≤40%	6 (3.3)	23 (2.2)	0.36			
Multivessel dilatation	13 (3.1)	24 (2.4)	0.45			
Number of stents per patient ≥ 2	22 (2.9)	15 (2.4)	0.53			
Total stent length > 36 mm	16 (2.5)	21 (2.8)	0.72			
Surgery within 60 days after SES implantation	6 (6.4)	31 (2.4)	0.02	1.68	1.03–2.52	0.04

ACS acute coronary syndrome, *HD* hemodialysis, *LAD* left anterior descending coronary artery, *LMCA* left main coronary artery, *LVEF* left ventricular ejection fraction, *SES* sirolimus-eluting stent, *STEMI* ST-segment elevation myocardial infarction

provisional BMS implantation instead of DES implantation in patients undergoing PCI who would be likely to require invasive or surgical procedures within 12 months [9]. However, several previous studies clearly demonstrated that preoperative coronary revascularization is not beneficial in many patients undergoing major vascular surgery [14, 15]. Those patients who truly need PCI before surgical procedures are considered to be a minority of patients undergoing surgical procedures. The present study clearly demonstrated that the need for surgical procedures

often develops after a DES has been implanted. It is our contention that the recommendation to avoid the use of DESs could hardly address the issues concerning surgical procedures after DES implantation. Furthermore, non-cardiac surgical procedures after BMS implantation have been reported to be associated with a high rate of perioperative ST and/or serious adverse events in the first 6 weeks after stent implantation [1–4]. Also, a meta-analysis comparing SES with BMS clearly demonstrated that the incidence and the timing of ST up to 1 year were not different between SES and BMS [16]. Therefore, if a given surgical procedure is truly required shortly after PCI, the choice of BMS seems not to provide much advantage over the choice of DES. Avoiding unnecessary PCI before surgical procedures is therefore much more important than the selection of the types of stent.

A report of three cases with perioperative ST late (343–442 days) after DES implantation highlighted the exaggerated ST risk after surgical procedures [5]. The reported incidences of ST of DES after surgical procedures ranged from 0 to 2% in several small series of patients [17–20]. A recent report of 481 patients undergoing surgical procedures after DES implantation showed ST (definite or modified probable) and composite of death, MI or ST at 30 days after surgery in 2.0 and 9.0% of patients, respectively [21]. The present study, which was evaluating the largest ever reported number of patients undergoing surgical procedures after DES implantation, suggested that surgical procedures are one of the risk factors for ST after SES implantation. The rate of ST at 30 days after surgical procedures (0.35%), seemed to be higher than the slope of the cumulative incidence curves of ST beyond 30 days (0.02% per month) in the entire j-Cypher registry cohort. The potential mechanisms for increased risk for ST appear to be related to discontinuation of antiplatelet therapy, activation of the sympathetic nervous system and the existence of a hypercoagulable state associated with surgery. However, the incidences of death/MI/ST (definite or probable) and ST (definite or probable) at 30 days after surgical procedures in this study were very low (2.7 and 0.35%, respectively) and reassuring. The lower incidence of adverse cardiac events as compared with the previous report [21] might be related to inclusion of minor surgeries in our study and generally low incidence of ST and other coronary events in the Japanese patient population [11].

Although the case report suggesting an increased risk of ST with DES highlighted the occurrence of ST late after DES implantation [5], several reports demonstrated that surgical procedures weeks after DES implantation were associated with an increased risk of adverse cardiac events [19, 21]. Our current result was consistent with those previous reports. Surgical procedures performed within 60 days after SES implantation as compared with those beyond 60 days carried a higher risk for adverse cardiac events including ST. A consensus statement from the American College of Cardiology and the American Heart Association recommended postponing elective surgery for at least 1 year in patients in whom a DES has been implanted [9]. Although the optimal duration of the delay is not yet known, duration shorter than 1 year would be appropriate considering the very low incidence of ST in patients with surgery beyond 60 days in the current study and the constant rate of occurrence of ST between 30 days and 3 years after DES implantation [8].

In the present study, we could not address the issue of optimal management of APT before and after surgical procedures. The incidences of adverse cardiac events including ST did not differ significantly according to the perioperative status of APT. This result was consistent with a previous study [21]. The risk of adverse cardiac events after surgical procedures are influenced by several factors other than the perioperative status of APT, including morbidities of patients, invasiveness of surgical procedures, timing of surgery after DES implantation and different lengths of time of discontinuation of APT. In real clinical practice, perioperative management of APT would have had been modified according to the risk factors that a given patient has. This would be the reason why we could not see clear differences in the rates of adverse cardiac events according to the perioperative status of APT.

However, optimal perioperative management of APT should certainly be better defined since this is the issue so frequently discussed in clinical practice. Since surgical procedures early after PCI were consistently reported to be associated with an increased risk for adverse cardiac events including ST, strict adherence to dual APT would be desirable up to 6 weeks to 2 months after PCI. Discontinuation of both aspirin and thienopyridine was reported to be associated with ST even beyond 1 year after DES implantation [11]. In a meta-analysis evaluating 50,279 patients at risk of or with coronary artery disease, aspirin non-adherence/withdrawal was reported to be associated with threefold higher risk of major adverse cardiac events [22]. In another meta-analysis involving 49,590 patients undergoing surgical procedures, aspirin increased the rate of bleeding complications by a factor of 1.5 (median, interquartile range: 1.0–2.5), but it did not lead to a higher level of the severity of bleeding complications [23]. Considering the risk and benefit profile of APT, it should be recommended to continue aspirin in most patients undergoing surgical procedures after DES implantation except for surgical procedures such as intracranial surgery and spinal surgery where serious clinical consequences are expected after bleeding. When discontinuation was unavoidable, it seems practically important to make the duration of discontinuation as short as possible, since the

majority of ST events were reported to have occurred beyond 1 week after discontinuation of APT [11]. Since bleeding time was reported to recover to the baseline level after 3–5 days of aspirin cessation, discontinuation of aspirin 3–5 days before surgical procedures would be long enough to minimize bleeding risk when discontinuation of aspirin is unavoidable [24, 25].

There are several important limitations of this study. First, surgical procedures constituting the study population were follow-up events in the j-CYPHER registry. Although we had extensive data on clinical, lesion and procedural characteristics at the time of the index PCI procedures, we did not collect detailed information on the surgical procedures such as the type of anesthesia, urgency of the surgical procedures and periprocedural bleeding complications. Therefore, analysis of the risk factors for the primary outcome measure was conducted based on baseline characteristics at the time of index PCI procedures. Secondly, we did not make systematic evaluation of electrocardiogram and cardiac biomarkers such as troponin to detect perioperative MI. This would be likely to underestimate the rate of perioperative MI. Thirdly, although data on surgical procedures during follow-up were prospectively collected in the j-Cypher registry, it is possible that the attending physicians in the cardiology division did not recognize and record details of all the surgical procedures conducted. This would be likely to underestimate the incidence of surgical procedures during follow-up. Finally, although data on discontinuation of APT were prospectively collected, it is possible that the surgeons might have discontinued APT without notice to the attending physicians in the cardiology division. Also, when follow-up information was obtained by contact with patients, information regarding discontinuation of APT was based on retrospective recall by the patients or relatives, suggesting a potential for recall bias. These factors would be likely to underestimate the prevalence of patients who discontinued APT before surgical procedures.

Conclusions

Despite these study limitations, we would conclude that surgical procedures were often required after PCI using SES (5% per year) and that the incidences of adverse cardiac events including ST after surgical procedures were acceptably low. Surgery within 60 days after SES implantation carried significantly higher risk as compared with those beyond 60 days.

Acknowledgments We are indebted to Ms. Natsuko Nakajo, Ms. Megumi Hirose, Ms. Mai Fujino and Ms. Hiromi Yoshida for their secretarial assistance. Funding sources include Cordis Cardiology Japan and Johnson and Johnson company.

Conflict of interest statement The authors have following relationship with the sponsor of the study: Takeshi Kimura and Takaaki Isshiki are advisory board members and in receipt of honoraria.

References

1. Kaluza GL, Joseph J, Lee JR, Raizner ME, Raizner AE. Catastrophic outcomes of non-cardiac surgery soon after coronary stenting. J Am Coll Cardiol. 2000;35:1288–94.
2. Wilson SH, Fasseas P, Orford JL, Lennon RJ, Horlocker T, Charnoff NE, et al. Clinical outcome of patients undergoing non-cardiac surgery in the 2 months following coronary stenting. J Am Coll Cardiol. 2003;42:234–40.
3. Sharma AK, Ajani AE, Hamwi SM, Maniar P, Lakhani SV, Waksman R, et al. Major non-cardiac surgery following coronary stenting: when is it safe to operate? Catheter Cardiovasc Interv. 2004;63:141–5.
4. Reddy PR, Vaitkus PT. Risks of non-cardiac surgery after coronary stenting. Am J Cardiol. 2005;95:755–7.
5. McFadden EP, Stabile E, Regar E, Cheneau E, Ong AT, Kinnaird T, et al. Late thrombosis in drug-eluting coronary stents after discontinuation of antiplatelet therapy. Lancet. 2004;364:1519–21.
6. Pfisterer M, Brunner-La Rocca HP, Buser PT, Rickenbacher P, Hunziker P, Mueller C, et al. Late clinical events after clopidogrel discontinuation may limit the benefit of drug-eluting stents: an observational study of drug-eluting versus bare-metal stents. J Am Coll Cardiol. 2006;48:2584–91.
7. Lagerqvist B, James SK, Stenestrand U, Lindbäck J, Nilsson T, Wallentin L, et al. Long-term outcomes with drug-eluting stents versus bare-metal stents in Sweden. N Engl J Med. 2007;356:1009–19.
8. Daemen J, Wenaweser P, Tsuchida K, Abrecht L, Vaina S, Morger C, et al. Early and late coronary stent thrombosis of sirolimus-eluting and paclitaxel-eluting stents in routine clinical practice: data from a large two-institutional cohort study. Lancet. 2007;369:667–78.
9. Grines CL, Bonow RO, Casey DE Jr, Gardner TJ, Lockhart PB, Moliterno DJ, et al. Prevention of premature discontinuation of dual antiplatelet therapy in patients with coronary artery stents: a science advisory from the American Heart Association, American College of Cardiology, Society for Cardiovascular Angiography and Interventions, American College of Surgeons, and American Dental Association, with representation from the American College of Physicians. Circulation. 2007;115:813–8.
10. Brilakis ES, Banerjee S, Berger PB. The risk of drug-eluting stent thrombosis with non-cardiac surgery. Curr Cardiol Rep. 2007;9:406–11.
11. Kimura T, Morimoto T, Nakagawa Y, Tamura T, Kadota K, Yasumoto H, et al. Antiplatelet therapy and stent thrombosis after sirolimus-eluting stent implantation. Circulation. 2009;119:987–95.
12. Serruys PW, Ong AT, van Herwerden LA, Sousa JE, Jatene A, Bonnier JJ, et al. Five-year outcomes after coronary stenting versus bypass surgery for the treatment of multi-vessel disease: the final analysis of the Arterial Revascularization Therapies Study (ARTS) randomized trial. J Am Coll Cardiol. 2005;46:575–81.
13. Cutlip DE, Windecker S, Mehran R, Boam A, Cohen DJ, van Es GA, et al. Clinical end points in coronary stent trials: a case for standardized definitions. Circulation. 2007;115:2344–51.
14. McFalls EO, Ward HB, Moritz TE, Goldman S, Krupski WC, Littooy F, et al. Coronary-artery revascularization before elective major vascular surgery. N Engl J Med. 2004;351:2795–804.

15. Poldermans D, Schouten O, Vidakovic R, Bax JJ, Thompson IR, Hoeks SE, et al. A clinical randomized trial to evaluate the safety of a non-invasive approach in high-risk patients undergoing major vascular surgery: the DECREASE-V pilot study. J Am Coll Cardiol. 2007;49:1763–9.
16. Kastrati A, Mehilli J, Pache J, Kaiser C, Valgimigli M, Kelbaek H, et al. Analysis of 14 trials comparing sirolimus-eluting stents with bare-metal stents. N Engl J Med. 2007;356:1030–9.
17. Compton PA, Zanker AA, Adesanya AO, Banerjee S, Brilakis ES. Risk of non-cardiac surgery after coronary drug-eluting stent implantation. Am J Cardiol. 2006;98:1212–3.
18. Kim HL, Park KW, Kwak JJ, Kim YS, Sir JJ, Lee SJ. Stent-related cardiac events after non-cardiac surgery: drug-eluting stent vs. bare metal stent. Int J Cardiol. 2008;123:353–4.
19. Schouten O, van Domburg RT, Bax JJ, de Jaegere PJ, Dunkelgrun M, Feringa HH, et al. Non-cardiac surgery after coronary stenting: early surgery and interruption of antiplatelet therapy are associated with an increase in major adverse cardiac events. J Am Coll Cardiol. 2007;49:122–4.
20. Brotman DJ, Bakhru M, Saber W, Aneja A, Bhatt DL, Tillan-Marthinez K, et al. Discontinuation of antiplatelet therapy prior to low-risk non-cardiac surgery in patients with drug-eluting stents: a retrospective cohort study. J Hosp Med. 2007;2:378–84.
21. Anwaruddin S, Askari AT, Saudye H, Batizy L, Houghtaling PL, Alamoudi M, et al. Characterization of post-operative risk associated with prior drug-eluting stent use. JACC Cardiovasc Interv. 2009;2:542–9.
22. Biondi-Zoccai GGL, Lotrionte M, Agostoni P, Abbate A, Fusaro M, Burzotta F, et al. A systematic review and meta-analysis on the hazards of discontinuing or not adhering to aspirin among 50,279 patients at risk for coronary artery disease. Eur Heart J. 2006;27:2667–74.
23. Burger W, Chemnitius M, Kneissl GD, Rucker G. Low-dose aspirin for secondary cardiovascular prevention—cardiovascular risks after its perioperative withdrawal versus bleeding risks with its continuation—review and meta-analysis. J Intern Med. 2005;257:399–414.
24. Sonksen JR, Kong KL, Holder R. Magnitude and time course of impaired primary haemostasis after stopping chronic low and medium dose aspirin in healthy volunteers. Br J Anaesth. 1999;82:360–5.
25. Komatsu T, Tamai Y, Takami H, Yamagata K, Fukuda S, Munakata A. Study for determination of the optimal cessation period of therapy with anti-platelet agents prior to invasive endoscopic procedures. J Gastroenterol. 2005;40:698–707.